AD-A175 945 HEAT TRANSFER FROM AN ARRAY OF HEATED CYLINDRICAL ELEMENTS OF AN ADIABATIC CHANNEL WALL(U) NAVAL POSTGRADUATE SCHOOL MONTEREY CA J D PIATT SEP 86 1/1

UNCLASSIFIED F/G 20/13 NL

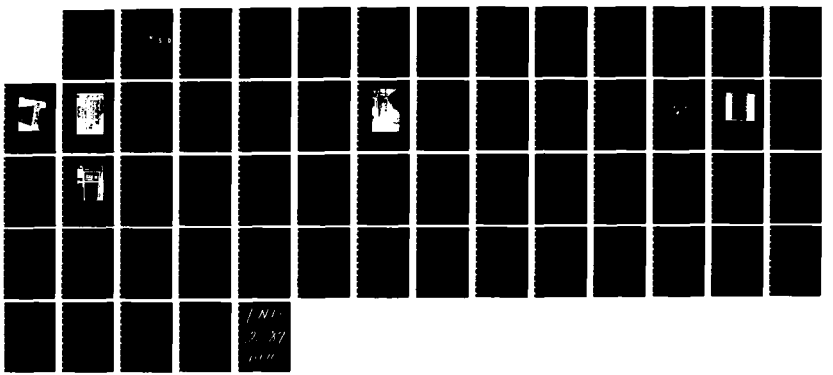

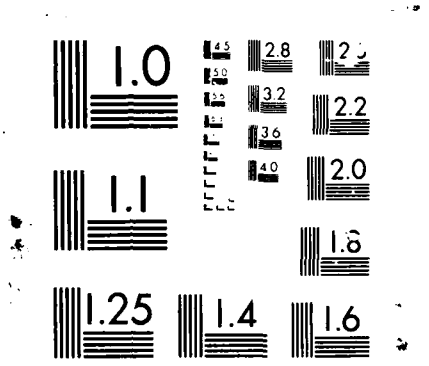
1.0
1.1
1.25
1.4
1.6
2.8
3.2
3.6
4.0
2.2
2.0
1.8

NAVAL POSTGRADUATE SCHOOL
Monterey, California

THESIS

HEAT TRANSFER FROM AN ARRAY OF
HEATED CYLINDRICAL ELEMENTS ON AN
ADIABATIC CHANNEL WALL

by

James D. Piatt, Jr.

September 1986

Thesis Adivsor: Allan D. Kraus

Approved for public release; distribution is unlimited.

UNCLASSIFIED
SECURITY CLASSIFICATION OF THIS PAGE

REPORT DOCUMENTATION PAGE

1a REPORT SECURITY CLASSIFICATION UNCLASSIFIED	1b RESTRICTIVE MARKINGS AD-A175 945
2a SECURITY CLASSIFICATION AUTHORITY	3 DISTRIBUTION / AVAILABILITY OF REPORT Approved for public release; distribution is unlimited
2b DECLASSIFICATION / DOWNGRADING SCHEDULE	
4 PERFORMING ORGANIZATION REPORT NUMBER(S)	5 MONITORING ORGANIZATION REPORT NUMBER(S)
6a NAME OF PERFORMING ORGANIZATION Naval Postgraduate School 6b OFFICE SYMBOL (If applicable) Code 69	7a NAME OF MONITORING ORGANIZATION Naval Postgraduate School
6c ADDRESS (City, State, and ZIP Code) Monterey, California 93943-5000	7b ADDRESS (City, State, and ZIP Code) Monterey, California 93943-5000
8a NAME OF FUNDING / SPONSORING ORGANIZATION 8b OFFICE SYMBOL (If applicable)	9 PROCUREMENT INSTRUMENT IDENTIFICATION NUMBER
8c ADDRESS (City, State, and ZIP Code)	10 SOURCE OF FUNDING NUMBERS PROGRAM ELEMENT NO / PROJECT NO / TASK NO / WORK UNIT ACCESSION NO

11 TITLE (Include Security Classification)
HEAT TRANSFER FROM AN ARRAY OF HEATED CYLINDRICAL ELEMENTS ON AN ADIABATIC CHANNEL WALL

12 PERSONAL AUTHOR(S)
Piatt, James D., Jr.

13a TYPE OF REPORT	13b TIME COVERED	14 DATE OF REPORT (Year, Month, Day)	15 PAGE COUNT
Master's Thesis	FROM _____ TO _____	1986 September	58

16 SUPPLEMENTARY NOTATION

17 COSATI CODES			18 SUBJECT TERMS (Continue on reverse if necessary and identify by block number)
FIELD	GROUP	SUB-GROUP	Heated cylindrical array; convective heat-transfer from cylinders; circuit board cooling; electronic cooling.

19 ABSTRACT (Continue on reverse if necessary and identify by block number)

This thesis describes an experimental study of the fluid dynamics and heat transfer characteristics of Laminar air flow across cylindrical elements mounted on one wall of a vertical adiabatic channel. Various combinations of approach velocity and channel widths were employed and the variations of the row by row heat transfer coefficients between elements of the array and the air stream were determined.

20 DISTRIBUTION / AVAILABILITY OF ABSTRACT ☒ UNCLASSIFIED/UNLIMITED ☐ SAME AS RPT ☐ DTIC USERS	21 ABSTRACT SECURITY CLASSIFICATION UNCLASSIFIED
22a NAME OF RESPONSIBLE INDIVIDUAL Prof. Allan D. Kraus	22b TELEPHONE (Include Area Code) (408) 646-649-8276 22c OFFICE SYMBOL Code 69Ks

DD FORM 1473, 84 MAR

83 APR edition may be used until exhausted
All other editions are obsolete

SECURITY CLASSIFICATION OF THIS PAGE
UNCLASSIFIED

Approved for public release; distribution is unlimited.

Heat Transfer From An Array of Heated Cylindrical Elements On An Adiabatic Channel Wall

by

James D. Piatt, Jr.
Lieutenant, United States Navy
B.A., State University of New York at Geneseo, 1980

Submitted in partial fulfillment of the
requirements for the degree of

MASTER OF SCIENCE IN MECHANICAL ENGINEERING

from the

NAVAL POSTGRADUATE SCHOOL
September 1986

Author: James D. Piatt, Jr.
James D. Piatt, Jr.

Approved by: Allan D. Kraus
Allan D. Kraus, Thesis Advisor

A. J. Healey
A. J. Healey, Chairman, Department of
Mechanical Engineering

John N. Dyer
John N. Dyer,
Dean of Science and Engineering

ABSTRACT

This thesis desc. ;es an experimental study of the fluid dynamics and heat transfer characteristics of Laminar air flow across cylindrical elements mounted on one wall of a vertical adiabatic channel. Various combinations of approach velocity and channel width were employed and the variations of the row by row heat transfer coefficients between elements of the array and the air stream were determined.

TABLE OF CONTENTS

LIST OF TABLES

LIST OF FIGURES

NOMENCLATURE

A	Surface area of cylinder exposed to free stream air, m^2.
b	y intercept.
C	Multiplication constant, dimensionless.
d	Diameter of cylindrical element, m.
e^+	Roughness Reynolds number based on e, a characteristic height of the roughness, dimensionless.
g^+	Heat transfer similarity function, dimensionless.
h	Local heat-transfer coefficient, W/m^2-°C.
H	Distance between channel splitter places m.
I	Current drawn, A.
k	Thermal conductivity of free stream air, W/m-°C.
L	Height of cylindrical element, m.
m	Slope of a line.
N	Row position number in array.
Nu_H	Nusselt number, hH/k.
Pr	Prandtl number, $C_p\mu/k$, dimensionless.
$\dot{Q}_{input}$	Power input from electrical power supply, W.
$\dot{Q}_{losses}$	Power lost from cylindrical elements, W.
Re_H	Reynolds number, HU_∞/ν, dimensionless.
$T_{s,o}$	Surface temperature of the cylinder heated by the resistor, °C.
$T_{s,i}$	Surface temperature of the ith cylinder heated by the thermal wake, °C.

T_∞ Freestream air temperature, °C.

U_∞ Freestream air velocity, m/s.

V Power supply voltage, V.

Greek Symbols

θ Dimensionless temperature of a cylinder in the same column as the cylinder heated by a resistor.

ν Kinematic viscosity, m^2/s.

ACKNOWLEDGEMENT

I would like to express my sincerest appreciation to the staff of the Mechanical Engineering Machine Shop for their timely efforts in the construction of and numerous modifications to the test apparatus.

To Professor Kraus, for his guidance, efforts and patience throughout the span of this endeavor, thank you for seeing me through it all.

To my wonderful wife, Cirille, for her moral support needed so often and for being my wife during these trying times --a very special thank you.

I. INTRODUCTION

The removal of heat from electronic equipment to assure reliable operation has been a problem plaguing the electronic industry for many years. As a result, many researchers have attempted to develop specific correlations to enable designers to attempt to predict possible solutions to this problem.

This research concerns air flowing across cylindrical elements mounted in an array on one wall of a vertical adiabatic channel. This configuration is much the same as an array of transistors in the TO5 configuration arranged on stacks of parallel circuit boards in various types of electronic equipment.

A. THEORY OF VERTICAL CHANNELS FORMED BY CIRCUIT BOARDS

Many electronic systems consist partially of arrays of printed circuit boards supporting a fairly dense array of electronic elements on one side as shown in Figure 1.1. These circuit boards can be arranged so that the side with the elements (front side) faces the relatively smooth backside of another. When a series of circuit boards are arranged in such a fashion (see Figure 1.2), long vertical channels in which cooling air can be supplied by forced convection can result. During operation, the elements such as flatpacks, dips resistors and transistors generate heat, the majority of which is dissipated to the surroundings with little transmitted back through the circuit board. As a result, it appears as if all of the heat is

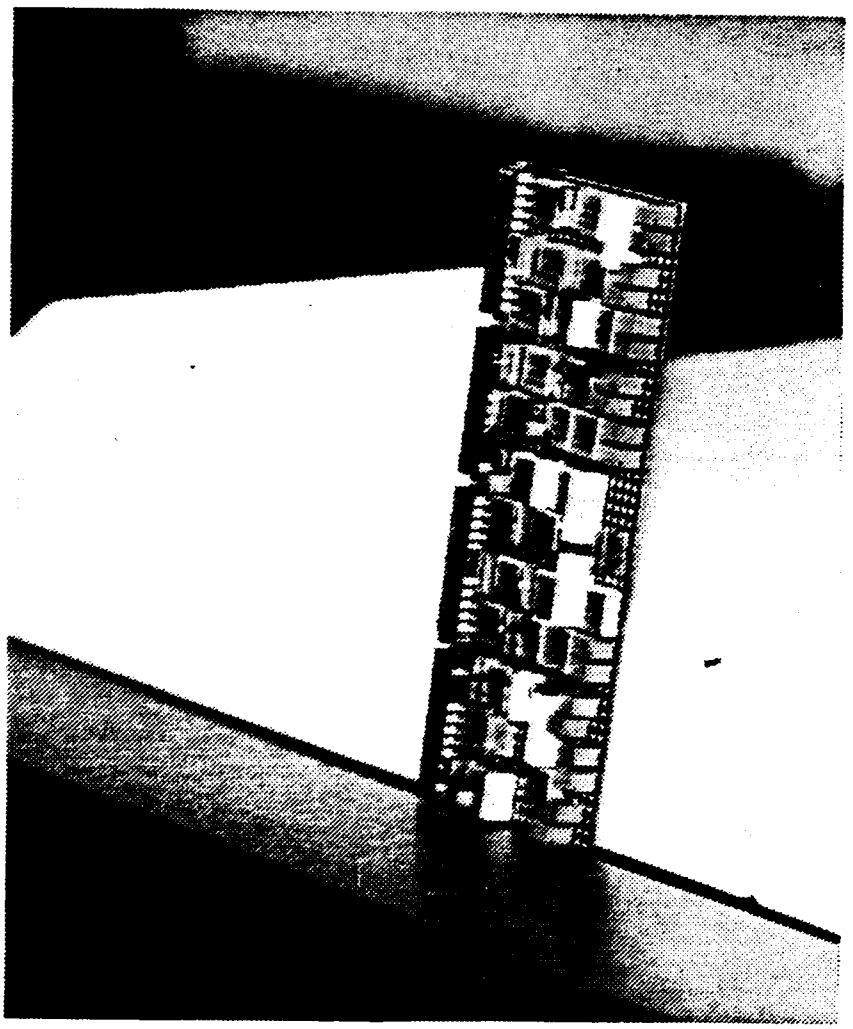

Figure 1.1 Modern Circuit Board

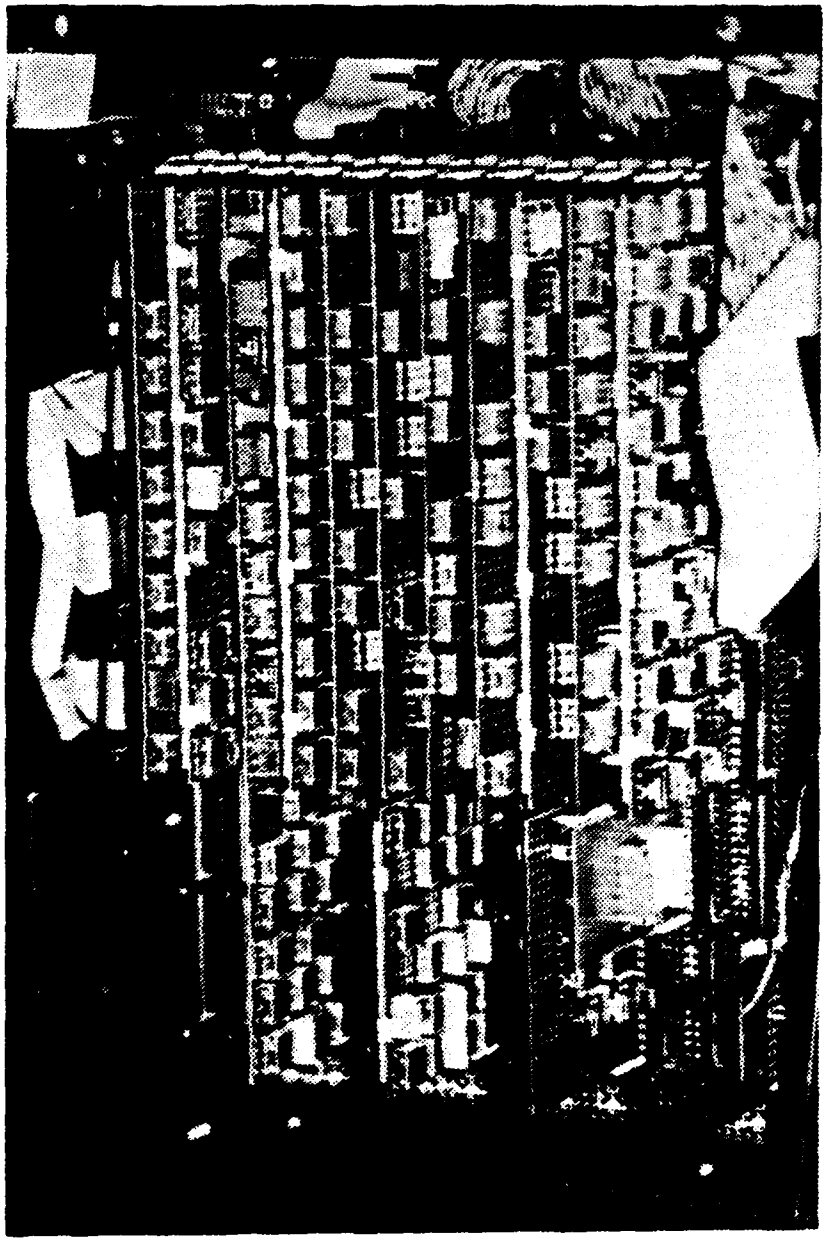

Figure 1.2 Modular Arrangement of Circuit Board

transmitted by one side of the channel or one side of each circuit board to the air stream or air layer between the boards.

Complexity is added to the system when elements serve different purposes and, as a result, possess different sizes, shapes and heat dissipating characteristics.

The process of heat removal from electronic systems creates a very comlex design problem governed by such factors as circuit board/element arrangement, spacing, heating characteristics and operating environment. Moreover, the ultimate goal of any thermal analysis and the prediction of operating temperatures is the assessment of reliability. Reliability is the probability that an electronic component/system will operate properly without failure for its intended lifetime under its environmental operating conditions. [Ref. 1]

For many years, there have been numerous attempts to derive techniques to aid designers in this field. Unfortunately, the methods developed are often too complex, inadequate or restricted to specific conditions.

Early work with natural convection between parallel arrays of vertical circuit boards was performed by Elenbaas [Ref. 2], Bodoia and Osterle [Ref. 3] and Engel and Muller [Ref. 4]. In 1972, Aung et al. [Ref. 5] studied the effects of circuit board supports and elements in the field of flow for wide channel spacings. Aung went on to investigate uniform heat flux on two channel walls in which he subsequently studied the effects of baffles and circuit board staggering. [Ref. 6] There is

considerable literature describing the efforts that have been made to attempt to model circuit channel cooling by natural convection and forced convection.

For example, Kelleher utilized a thermal network approach to derive a more representative model of forced convection for one specific geometry with equal heat releases [Ref. 7]. Other experimental or semi-experimental approaches were performed by Tamura [Ref. 8], Finch [Ref. 9], Laermer [Ref. 10], Marto [Ref. 11] and Parkes and Preston [Ref. 12]. Most of this work is restricted to specific conditions.

B. THEORY OF SURFACE ROUGHNESS GEOMETRIES

Surface roughnesses have been classified by several different techniques of which the most commonly used are the k and d type roughness classifications consisting of 2 and 3 dimension classes which are further divided into artificial and commercial roughness subclasses. Although many researchers allude to these classifications, only a limited number actually use this terminology in agreement. It is further noted that in the area of heat-transfer, the k- and d- type roughnesses seem irrelevant because the same heat transfer roughness parameter (g^+) correlation is proposed for all types of roughnesses.

C. THEORY OF HEAT TRANSFER FROM ROUGH SURFACES

Earlier researchers in this field seem to agree that the heat-transfer roughness parameter (g^+), commonly referred to as

the inverse of the sublayer Stanton number, takes the functional form:

$$g^+ = 1/St_{sublayer} = C(e^+)^p (Pr)^q$$

where e^+ is the roughness Reynolds number based on an arbitrary characteristic height of the roughness (e). The different values of p and q fall into two categories:

1. The assumption of similarity near the wall which results in value of p = .2 and q = .44 or for the eddy-diffusivity models p = .25 and q = .66 [Refs. 13 and 14].

2. The assumption of a breakdown in close to the wall similarity results in values of p = .45 and q = .57 or p = .5 and q = .66 for the eddy diffusivity models [Refs. 15 and 14].

With regard to this study, the foregoing is only of academic interest because the geometry here is defined as an in-line array of cylindrical elements.

II. EQUIPMENT DESIGN AND INSTRUMENTATION

The equipment utilized in this research was either manufactured by the Engineering Machine Shop or supplied by the Naval Engineering Department of the Naval Postgraduate School, Monterey, California.

A. WIND TUNNEL

The wind tunnel (Figure 2.1) is constructed of 1/8" plexiglass with the exception of two 1/4" access plates and various reinforcement members mounted on the exterior so as to ensure smooth air flow on the tunnel interior.

The test section of the tunnel has a 12" by 4" cross section and a height of 18" with access covers on both faces to facilitate instrumentation and support for the test surfaces.

The tunnel intake is belled with an 18" radius to produce an orifice that has a 40" by 12" cross section. An adjustable leg is attached at each corner to serve as a support for the tunnel, to level the tunnel and to provide an 8" clearance off the floor.

The upper end of the tunnel is reduced to a section of 2" PVC ducting which is connected to a 550 cfm turbo fan. Air flow through the tunnel is controlled by a series of valves connected in line with the fan.

A 1/8" plexiglass splitter plate was mounted 1/2" off of the access plate facing the test surface in order to reduce the effects of the boundary layer formed in the tunnel. This

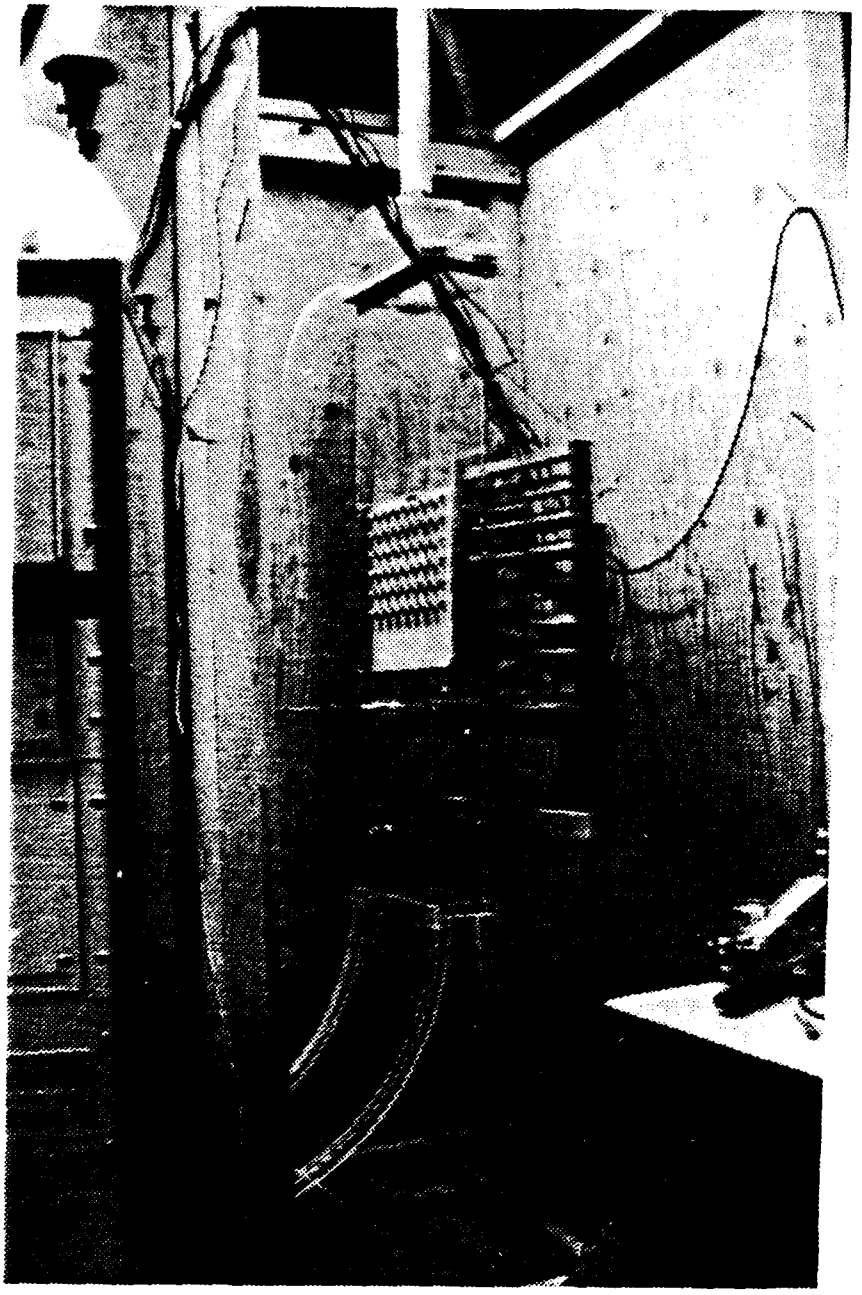

Figure 2.1 Photograph of Wind Tunnel.

distance was pre-determined through the use of computer software [Ref. 16] and the results are displayed in Figure 2.2. A wooden frame box (4'x4'x 8') was constructed around the wind tunnel to elliminate the effects of incident radiation on the cylinders from the laboratory environment and the box also served to reduce any transient air currents created by movement in the room (i.e., doors opening and closing).

B. TEST SURFACE

The design of the test surface used in this research was derived from the previous work of Arvizu and Moffat [Ref. 17] and Ortega [Ref. 18]. It was constructed of a 12" x 12.5" x 1/8" sheet of plexiglass (for support) with a 12" x 12.5" x 3/8" sheet of balsa wood (thermal boundary) cemented to it. The leading edge of this (balsa wood-plexiglass) splitter plate was cut at a 35° angle to form a sharp leading edge to reduce the effects of leading edge separation. The surface (balsa wood) of the splitter plate was then sanded and painted three times with white enamel paint and sanded a fourth time to ensure a smooth test surface. Small (1/16" diameter) holes were drilled through the plate to permit the installation of resistor leads and thermocouples into the cylindrical elements mounted on the balsa wood. Three mounting screws were attached to the plexiglass side of the splitter plate and to the access plate to facilitate the positioning of the test surface. A tail fin mounted to the tail end of the splitter plate was used to regulate the air flow on

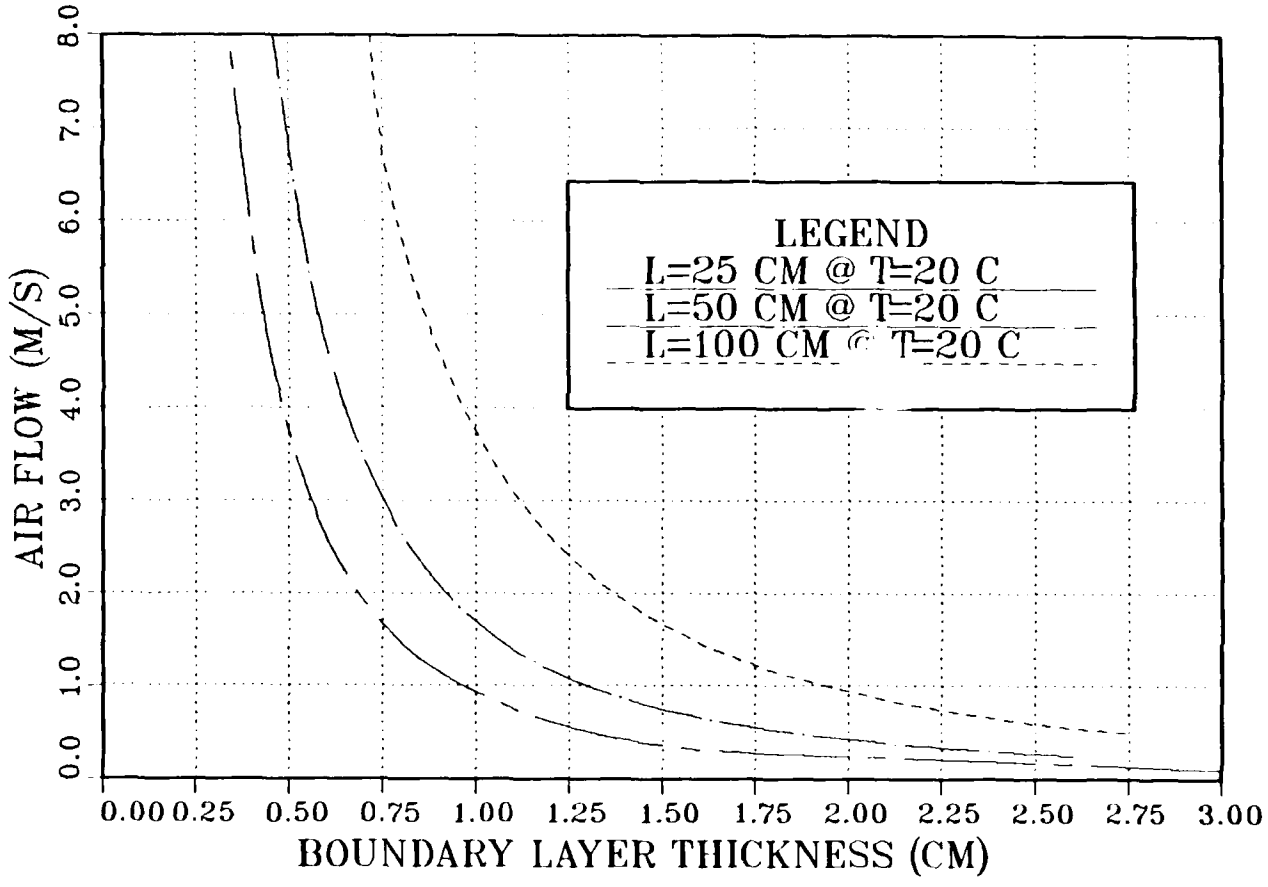

Figure 2.2 Approach Velocity vs. Boundary Layer Thickness for Various Channel Lengths.

both side of the splitter plate. A fourth adjusting screw was attached to this fin and through the access plate (Figure 2.3).

C. CYLINDRICAL ELEMENTS

The cylindrical elements used in this research were manufactured from 3/4" round aluminum stock and cut to a height of 1.0 cm. A 7/16" diameter hole was cut to a depth of 1/4" in the center of the element and two additional holes (1/8" diameter, 1/4 deep) were cut opposite each other to permit the installation of the 56 ohm, 1/2 watt resistors. Another hole (1/32" diameter, 3/8" deep) was drilled to position the thermocouple (Figure 2.4).

The resistors were epoxied into forty two of the cylinders and six more were cut in half so that an array of 7x6 cylinders could be mounted evenly on the splitter plate and the 12 half cylinders could be arranged along the edges of the plates (Figure 2.5).

The resistor (56 ohm, 1/2 watt), prior to insertion into the cylinders, had the leads cut and smaller leads (2841/1, #30 solid spc.) attached so as to reduce heat losses by conduction through them.

The cylinders were mounted on the test surface in an in-line array with a separation of one cylinder diameter between cylinders. This was done both vertically and horizontally.

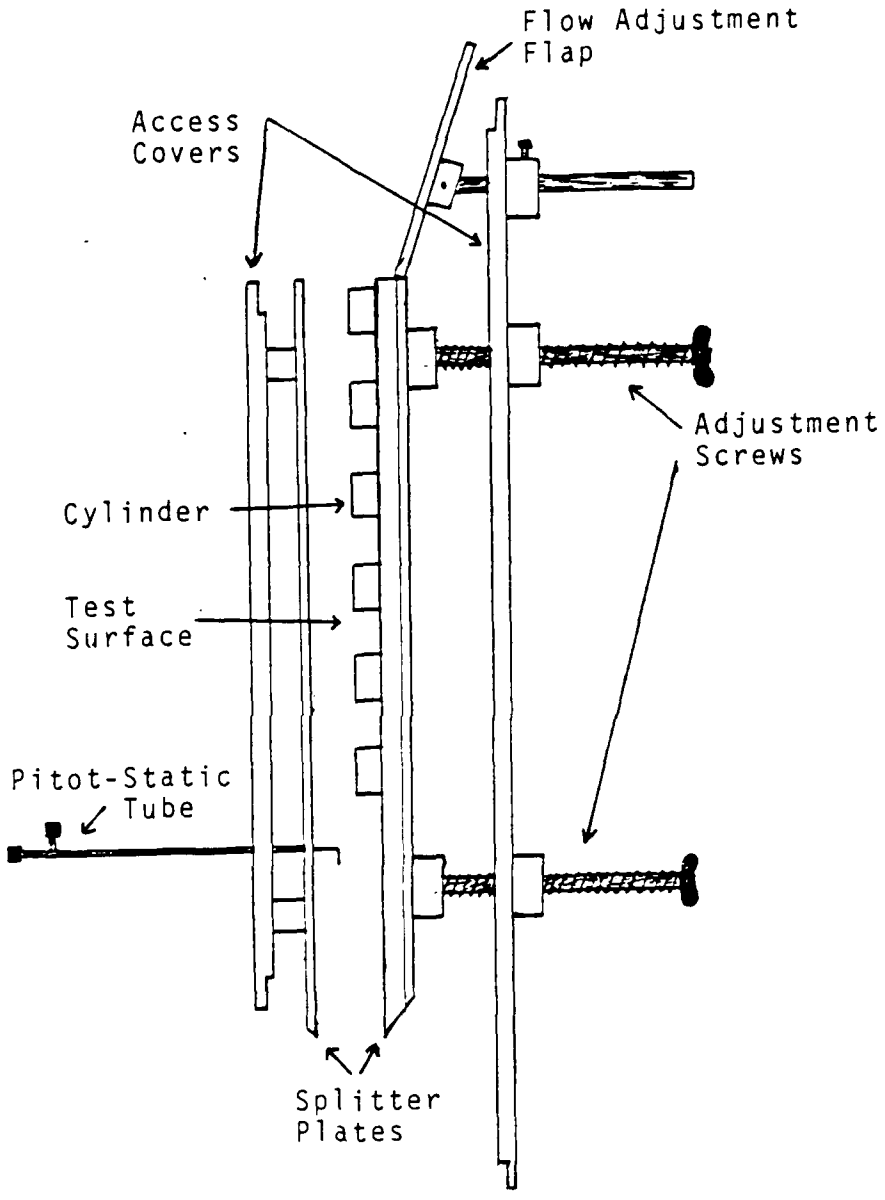

Figure 2.3 Sketch of Test Surface Configuration.

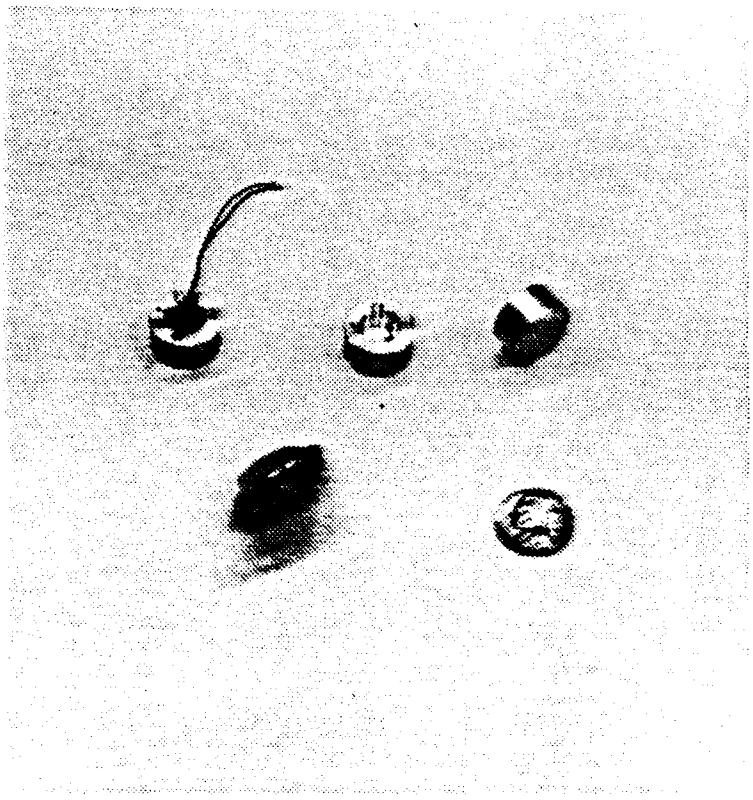

Top Row: Assorted Views of Cylinders
Bottom Row: TO5 Transistor and a nickel

Figure 2.4 Photograph of Cylinders.

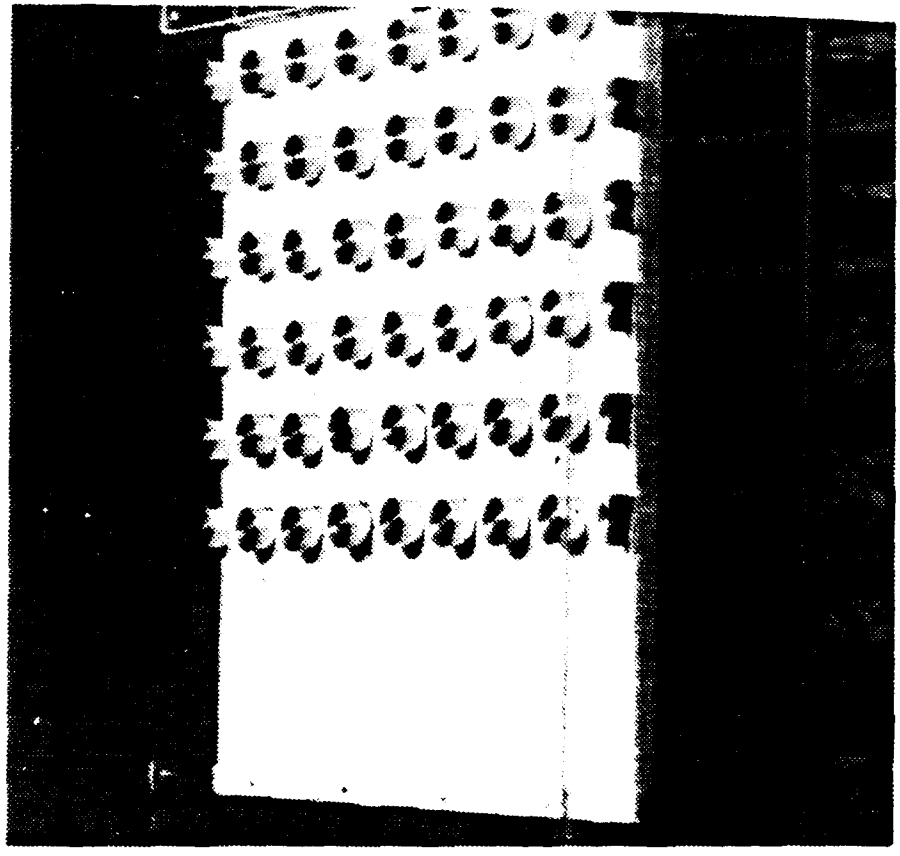

Figure 2.5 Photograph of Cylinders Arranged in an Array on the Test Surface.

D. INSTRUMENTATION

1. Temperature Measurements

Type T, copper-constantan thermocouples were utilized for the determination of the temperature of the heated elements and the inlet and outlet temperatures of the wind tunnel near the test surface. The thermocouples were connected to seven scanner boards in an autodata nine and calibrated to an accuracy of $\pm$0.2°F (Appendix A.) The thermocouples were then routed through an access plate in the tunnel through the splitter plate and into each of the elements.

2. Velocity Measurements

The velocity measurements were obtained by the use of a micro manometer and a pitot-static tube. Changes in the dynamic and static pressure were measured by the micro manometer and using Barnoulli's equation, velocity was determined. The pitot-static tube was placed between the splitter plate and the test surface splitter plate and used to determine the approach velocity between them.

A TSI (Model 1050/1050AA) hot wire anemometer was used to determine the velocity profile prior to entry into the test area. The hot wire anemometer was calibrated with the micro manometer and used only to ensure that the approach velocity was uniform.

Accuracy of the mirco manometer was determined to be $\pm$.0005 inches of water and resulted in an error of $\pm$0.2 ft/sec or $\pm$7cm/s. Because the micro manometer was utilized for the

calibration of the hot wire anemometer, more accuracy might result if the micro manometer was used to determine the velocity between the splitter plates.

3. Power Measurements and Control

A LAMBDA (60 volt, 10 amp) Regulated Power Supply (Model LK 345AFM) was used to power to the 56 ohm, 1/2 watt resistors mounted in the forty two cylindrical elements.

A switch board was set up to allow power to be delivered to individual elements in either of two columns, the third or the fourth columns. It was also set up in such a manner that each or all rows could be energized.

A Hewlett Packard digital multimeter (3466A) was used to measure the voltage drop across the resistors and a Fluke 8060A multimeter was used to measure the current through the circuit. The power delivered is the product of current and voltage.

4. Data Acquisition

The Autodata Nine mentioned above is a self contained recording device with up to 100 channels available for both temperature and voltage measurements. During this research, 71 channels were utilized, one for voltage measurement and the rest for temperature measurements in degrees Fahrenheit. (Figure 2.6)

E. EXPERIMENTAL PROCEDURE

For this research, data was recorded at three different channel height to cylinder height ratios (1.0, 2.3 and 4.6) for two different approach velocities (1.5 m/s and 3.0 m/s). The

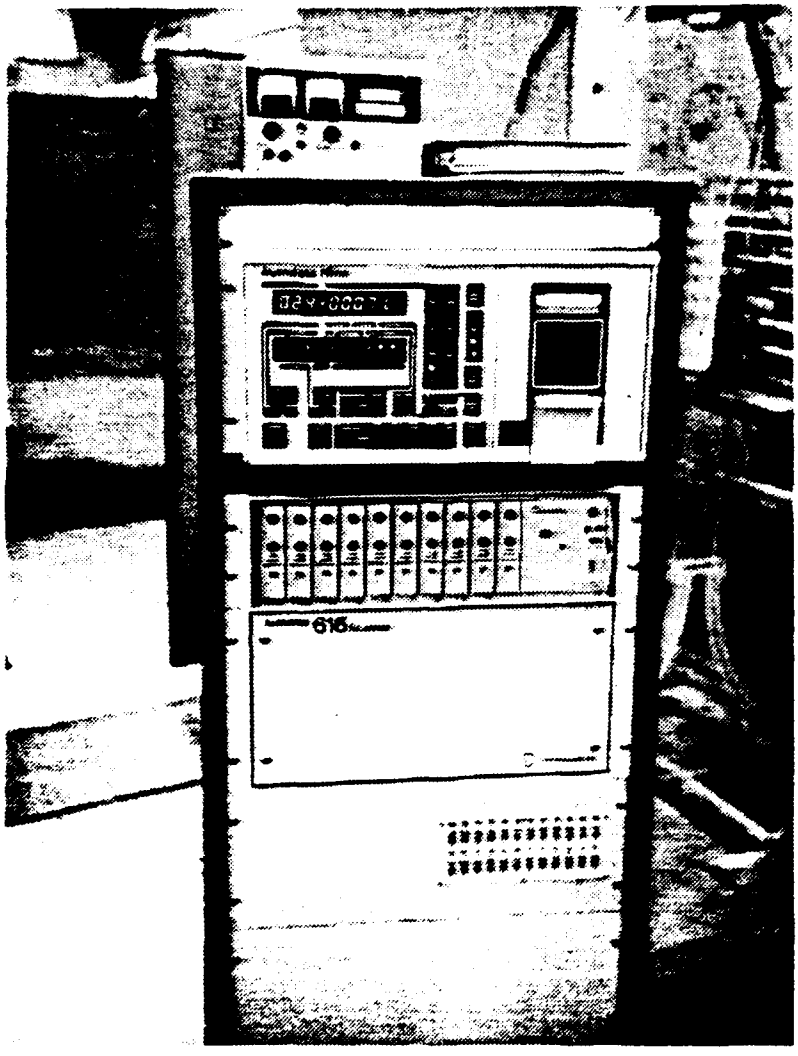

Figure 2.6 Photograph of Autodata Nine.

data recorded consisted of the voltage supplied to the circuit, the current through the circuit and the temperatures of the test elements as well as the inlet and exhaust temperatures of the airstream. For each channel height and approach velocity, data was gathered after a steady state condition was reached, for each element of a column energized one at a time and for the first four rows and for all six rows energized all at once.

III. DATA REDUCTION

A. DATA TAKEN

Inlet Free Stream Temperature, T_∞ (°F)

Cylinder Surface temperature, $T_{s,o}$ (°F)

Atmospheric Pressure, P_{atm} (inches Hg.)

Pitot-Static Pressure Difference, ΔP (inches H_2O)

Power Supply Voltage, V (volts)

Current Drawn, I (amps)

$T_{s,i}$ (°F)

B. SOUGHT AFTER PARAMETERS

1. Dimensionless Temperature Ratio

The Dimensionless Temperature Ratio, θ, is obtained as a function of cylinder location, channel configuration and freestream velocity. Here θ is defined as

$$\theta_i \triangleq \frac{T_{s,i} - T_\infty}{T_{s,1} - T_\infty}$$

where $T_{s,1}$ is the surface temperature obtained by the first passive cylinder directly after the cylinder heated by a resistor. $T_{s,i}$ is the surface temperature obtained by individual passive cylinders after and in the same column as the cylinder heated by the resistor where i is the row after the heated cylinder. Note that

$$\theta_1 = \frac{T_{s,1} - T_\infty}{T_{s,1} - T_\infty} = 1.0 \text{ by definition}$$

2. Heat-transfer Coefficient

The Heat-transfer Coefficient, $h(W/m^2{}^\circ C)$, is found and is a function of the cylinder location, channel configuration and freestream air velocity.

The heat transfer coefficient was determined as follows:

$$h = \frac{\dot{Q}_{input}\ (W) - \dot{Q}_{losses}\ (W)}{A\ (T_{s,o} - T_\infty)}$$

$T_{s,o}$ and T_∞ were recorded by the autodata nine and corrected by the calibration data in Appendix A.

A, is the surface area of the cylinder is calculated for channel/cylinder height ratios of 1.0, 2.3 and 4.6. If the channel/cylinder height ratio is equal to 1.0, $A = \pi dL$ and if the channel/cylinder height ratio is greater than 1.0, $A = \pi[dL + d^2/4]$.

The value of Q_{losses} in watts is derived from a parabolic temperature dependent approximation utilized by Ortega [Ref. 18] in his researach with aluminum cubes. This approximation is assumed to be the same for cylinders and is used here.

$$\dot{Q}_{losses}\ (W) = -0,62927 \times 10^{-3} + 0.5059 \times 10^{-2}(T_{s,o}-T_\infty) - 0.023695 \times 10^{-5}\ (T_{s,o}-T_\infty)^2$$

Ortega also determined the radiation losses to be an order of magnitude smaller than those given above, and radiation losses were therefore disregarded.

$\dot{Q}_{input}$(W) is the product of power supply voltage and current drawn.

$$\dot{Q}_{input} = V(volts) \times I(amps)$$

3. Reynolds Number

The Reynolds number is developed as a function of channel configuration and free stream air velocity. In this research, the Reynolds number was calculated using the freestream air velocity, channel height and viscosity as follows:

$$Re_H = \frac{\text{channel height x velocity}}{\text{viscosity}}$$

The value of the viscosity is obtained by a linear interpolation of data from tables of viscosity and air temperature.

4. Nusselt Number

The Nusselt number is prescribed as a function of channel configuration. Here, the Nusselt number was calculated using channel height, heat-transfer coefficient and the thermal conductivity of the free stream air as follows:

$$Nu_H = \frac{\text{channel height x heat-transfer coefficient}}{\text{thermal conductivity}}$$

The value of the thermal conductivity was obtained by a linear interpolation of data from tables of thermal conductivity and air temperature.

C. TYPICAL SET OF DATA

Table I presents a typical set of data obtained. These data will be used here to illustrate the data reduction procedure.

TABLE I

DATA SET

P_{atm} = 29.736 inches Hg.

ΔP = 0.0051 inches H_2O

Channel/Cylinder Height Ratio = 4.6

Cylinder Heated - row 1, column 3

Cylinder Surface Temperature, $T_{s,0}$ = 206.1°F

Voltage Supplied = 14.380 volts.

Current Drawn = 0.225 amps.

$T_{s,1}$ = 80.3°F
$T_{s,2}$ = 74.0°F
$T_{s,3}$ = 72.2°F
$T_{s,4}$ = 71.5°F
$T_{s,5}$ = 70.8°F
T_{∞} = 68.6°F

D. CALCULATIONS

1. Dimensionless Temperature Ratio,

The temperatures for the cylinder surface were recorded by the autod.ta nine and corrected by use of the thermocouple calibration data presented in Appendix A.

$T_{s,i}$ (corrected) = m x $T_{s,i}$ (recorded) - b

m	Recorded	b	$T_{s,i}$(Corrected)
$T_{s,1}$ =	1.0026 (80.3)	- 0.9038 =	79.6 °F

$T_{s,2} = 0.99994\ (74.0) - 0.19287 = 73.8\ ^{\circ}F$

$T_{s,3} = 1.0018\ \ (72.2) - 0.05645 = 72.3\ ^{\circ}F$

$T_{s,4} = 1,0018\ \ (68.6) - 0.5980 = 68.1\ ^{\circ}F$

$$\theta_i = \frac{T_{s,i} - T_\infty}{T_{s,1} - T_\infty}$$

$$\theta_1 = \frac{79.6 - 68.1}{79.6 - 68.1} = \frac{11.5}{11.5} = 1.0 \text{ (by definition)}$$

$$\theta_2 = \frac{73.8 - 68.1}{79.6 - 68.1} = \frac{5.7}{11.5} = 0.4956$$

$$\theta_3 = \frac{72.3 - 68.1}{79.6 - 68.1} = \frac{4.2}{11.5} = 0.3652$$

$$\theta_4 = \frac{71.2 - 68.1}{79.6 - 68.1} = \frac{3.1}{11.5} = 0.2696$$

$$\theta_5 = \frac{70.3 - 68.1}{79.6 - 68.1} = \frac{2.2}{11.5} = 0.1913$$

2. Heat-Tansfer Coefficient

$$h = \frac{\dot{Q}_{input} - \dot{Q}_{losses}}{A\ (T_{s,0} - T_\infty)}$$

$T_{s,0} = 1.0025\ (206.1^{\circ}F) - 0.4745 = 206.1^{\circ}F$ (corrected)

$T_{\infty} = 1.0018\ (68.6^{\circ}F) - 0.5980 = 68.1^{\circ}F$ (corrected)

$T_{s,0} - T_{\infty} = 206.1 - 68.1 = 138.0^{\circ}F = 76.7^{\circ}C$

Channel/cylinder height ratio = 4.6

therefore $A = -[(0.019m)\ (0.01m) + (0.019m)^2/4]$

$A = 0.00088 m^2$

$\dot{Q}_{losses} = 0.6927 \times 10^{-3} + 0.5059 \times 10^{-2}(T_{s,o}-T_\infty) - 0.23695 \times 10^{-6}(T_{s,o}-T_\infty)^2$

where $T_{s,o} - T_\infty$ is in $^\circ C$ and $\dot{Q}_{losses}$ is in watts.

$T_{s,o}-T_\infty = 76.7^\circ C$

$\dot{Q}_{losses} = 0.373$ watts

$\dot{Q}_{input} = VxI = 14.380$ volts x 0.225 amps = 3.27 watts

$$h = \frac{3.27 - 0.373}{0.00088\ (76.7)} = 42.92\ W/m^2\ ^\circ C$$

3. Reynolds Number

$Re_H = HU_\infty / \nu$

$H = 4.6\ (.01m) = 0.046m$

$U_\infty = 1.5 m/s$

$= 38.02 \times 10^{-6} - 109.8 \times 10^{-9}\ (27.0 - T_\infty)$

where T_∞ is in $^\circ C$

$T_\infty = 20.0^\circ C$

$= 38.02 \times 10^{-6} m^2/s$

$$Re_H = \frac{.046m \times 1.5 m/s}{38.02 \times 10^{-6} m^2/s} = 1814.7$$

4. Nusselt Number

$Nu_H = Hh/k$

$H = .046m \qquad h = 42.92\ W/m^2 ^\circ C$

$k = 0.0407 - 76.8 \times 10^{-6}\ (27.0-T_\infty)$

where T_∞ is in $^\circ C$

$k = 40.162 \times 10^{-3} w/m^\circ C$

$$Nu_H = \frac{.046m \times 42.92\ W/m^{2\circ}C}{40.162 \times 10^{-3}\ W/m^\circ C} = 49.16$$

IV. RESULTS

The experimental measurements that were obtained lead to two different subject categories: thermal wake effects and heat-transfer coefficient. Table II presents the range of the parameters covered and a listing of the data is tabulated in Appendix C.

TABLE II

PARAMETERS TESTED

Thermal Wake			
Channel Height/Cylinder Height Ratio	1.0		4.6
Downstream Row Number	0,1,2,5		0,1,2,5
Velocity (m/s)	1.5, 3.0		1.5, 3.0
Heat-Transfer Coefficient			
Channel Height/Cylinder Height Ratio	1.0	2.3	4.6
Heated Cylinder Row Number	1,2,3,6	1,2,3,6	1,2,3,6
Number of Rows Heated	4,6	4,6	4,6
Velocity (m/s)	1.5, 3.0	1.5, 3.0	1.5, 3.0

A. THERMAL WAKE

The thermal wake created by a single heated cylinder in an array is influenced by the channel height to cylinder height ratio, the mass flow rate and the position of the cylinder in the array.

For a channel height/cylinder height ratio of 1.0, there, is no free stream, and the flow through the array undergoes periodic accelerations and decelerations. It therefore seems unlikely

that a channel height/cylinder height ratio of 4.6 would possess the same convective means for determination of the downstream wake. However, a plot of δ as a function of downstream row number (Figure 4.1 and 4.2) demonstrates a 1/N dependence for both velocities at both channel heights.

Figure 4.3 shows an even closer resemblance to the 1/N curve for the thermal wake created by a heated cylinder located in a row internal to the matrix of cylinders.

The following is provided for the understanding of the graphical curves found in the legends of various graphs in Chapter IV:

Hx.xRxVx.x

Hx.x	Channel Height/Cylinder Height Ratio x.x
Rx	Row that the heated cylinder is in x
Vx.x	Approach Velocity x.x

For example, H.4.6R1V3.0 denotes data gathered at a channel height/cylinder height ratio of 4.6, where the cylinder heated is in the first row and the approach velocity is 3.0 m/s.

B. HEAT-TRANSFER COEFFICIENT

In Figure 4.4 the heat-transfer coefficient, h, for a single heated cylinder in the first row is plotted against channel height/cylinder height ratios for approach velocities of 1.5 m/s and 3.0 m/s. It can be seen that as the channel height increases, the value of h drops off fairly rapidly to an asymototic limit at a channel height/cylinder height ratio of

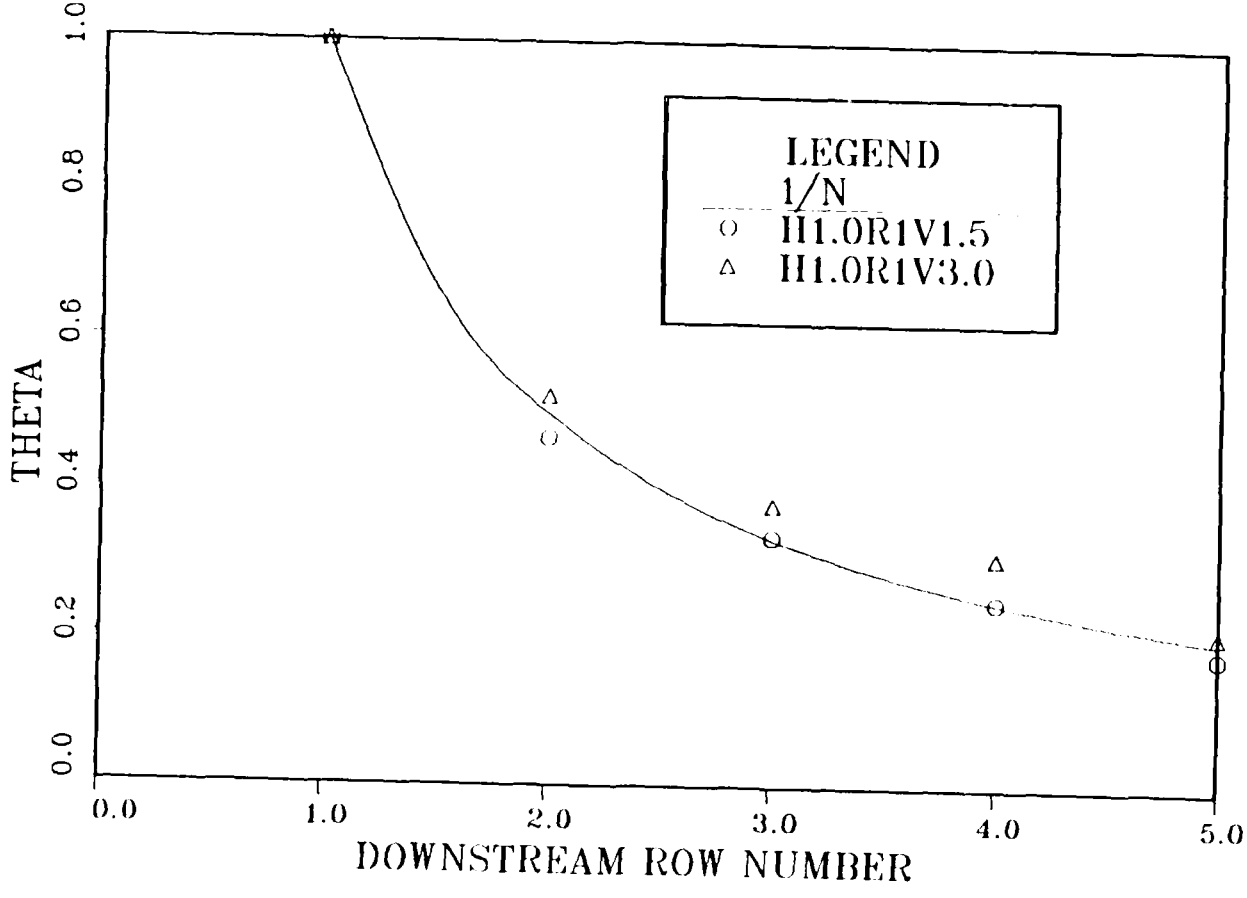

Figure 4.1 Normalized Dimensionless Temperature vs. Row Position for a Channel Height/Cylinder Height Ratio of 1.0 With Heated Element in the First Row.

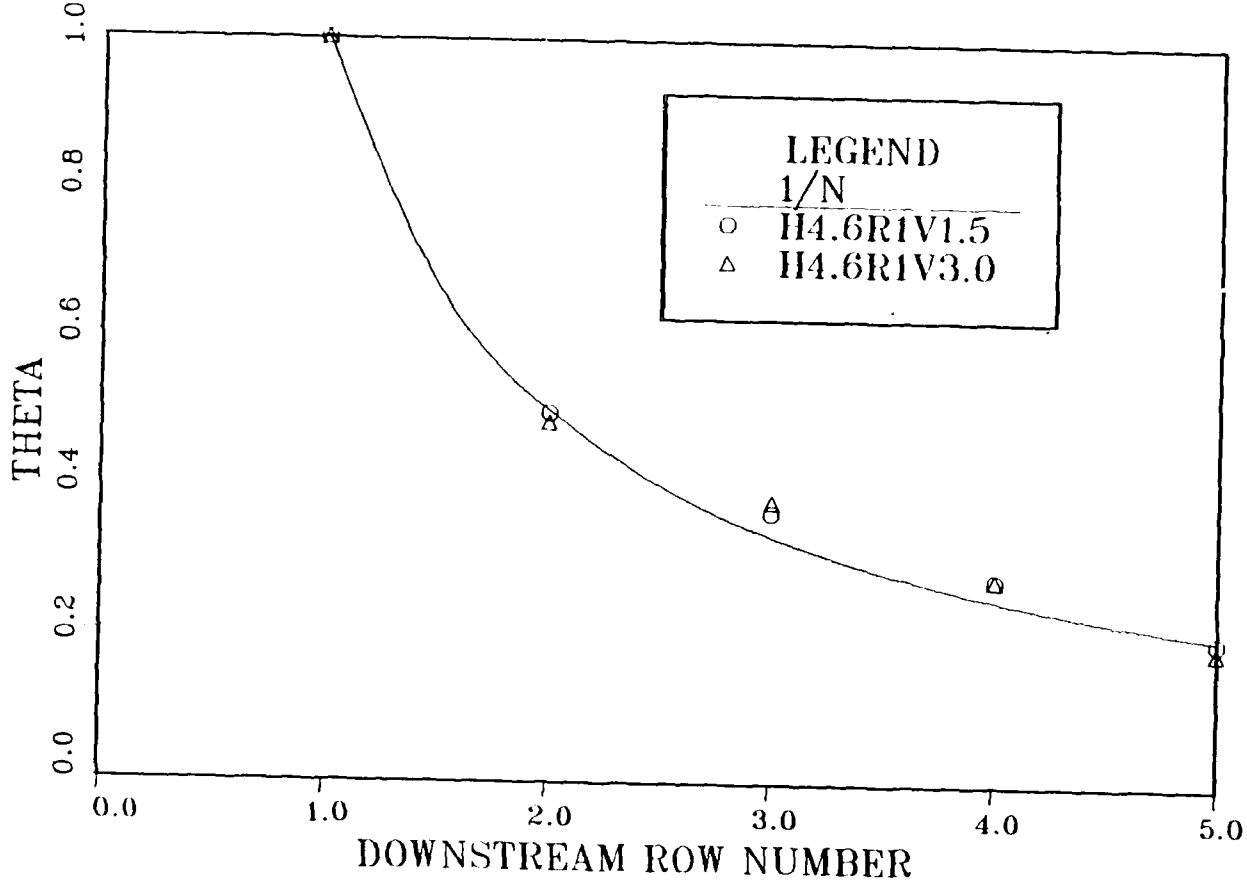

Figure 4.2 Normalized Dimensionless Temperature vs. Row Position for a Channel Height/Cylinder Height Ratio of 4.6 and Heated Element in the First Row.

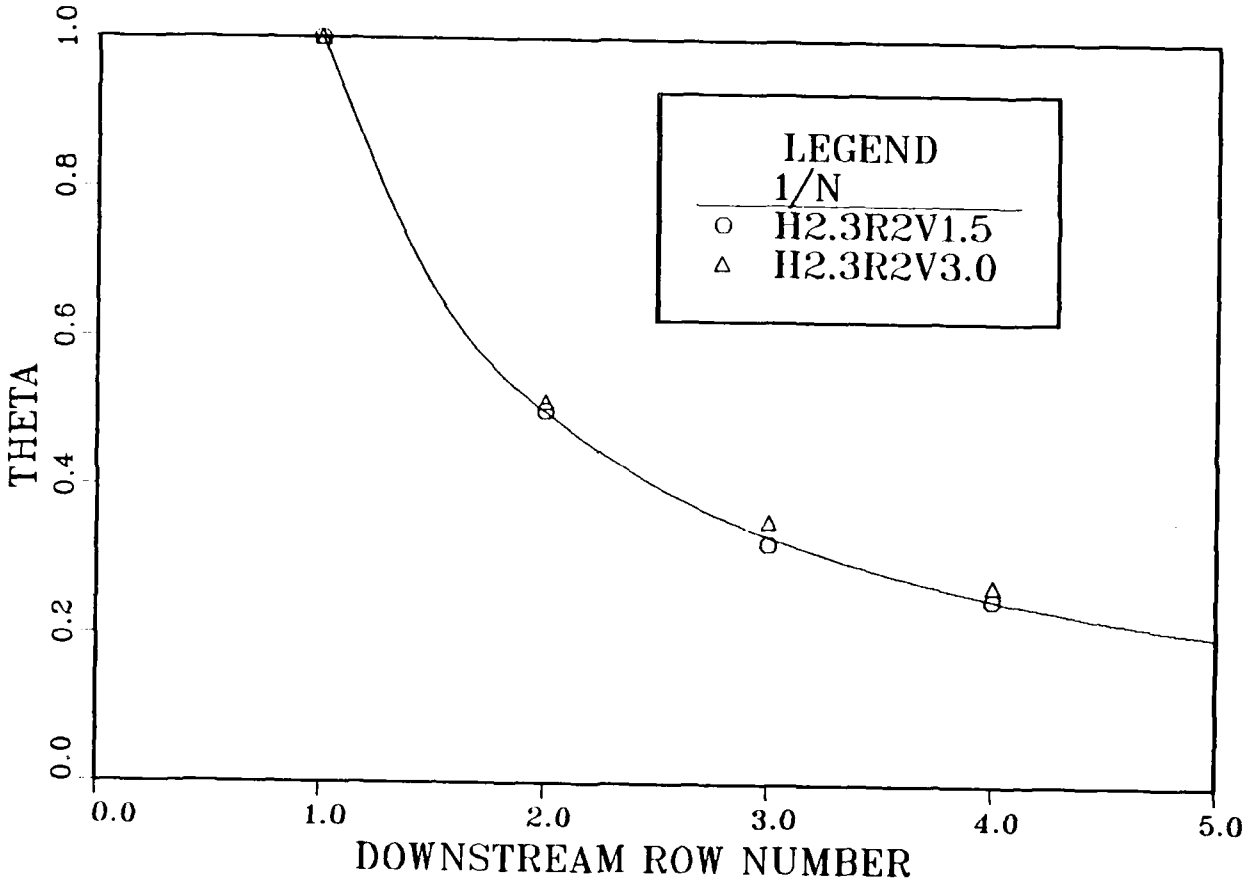

Figure 4.3. Normalized Dimensionless Temperature vs. Row Position for a Channel Height/Cylinder Height Ratio of 2.3 and Heated Element in the Second Row.

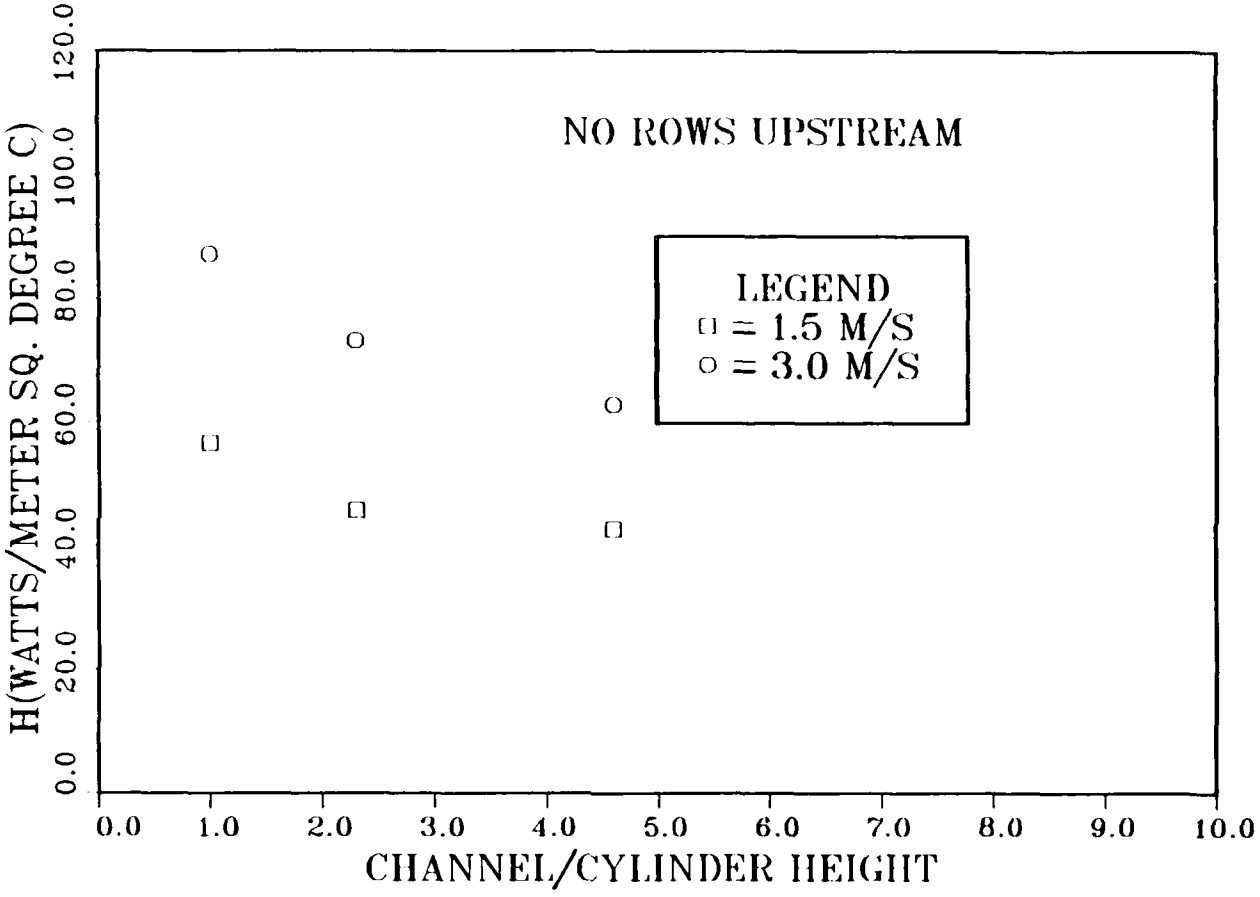

Figure 4.4 Heat-transfer Coefficient vs. Channel Height/ Cylinder Height Ratio With No Rows Upstream

4.6. Air flows over the cylinders instead of through them (the path of least resistance).

Figure 4.5 show a plot of h against the channel height to cylinder height ratio for an internal cylinder where h drops off a little more rapidly.

Figure 4.6 plots h against array position for a channel height/cylinder height ratio of 1.0. Here, h increases with position upstream. This correlates to the increased turbulence with position downstream.

Figure 4.7 is a plot of h against array position for a channel height to cylinder height ratio of 4.6. For this configuration h appears to increase slightly and then drop off slightly so that the value of h at the sixth row is less then that of the first row.

Figure 4.8 plots Nusselt number against Reynolds number for all three channel height to cylinder height ratios. This composition leads to a correlation of the form $Nu = C\ Re^{0.55}$ where C is different for different array densities as noted by Arvizu and Moffat [Ref. 17].

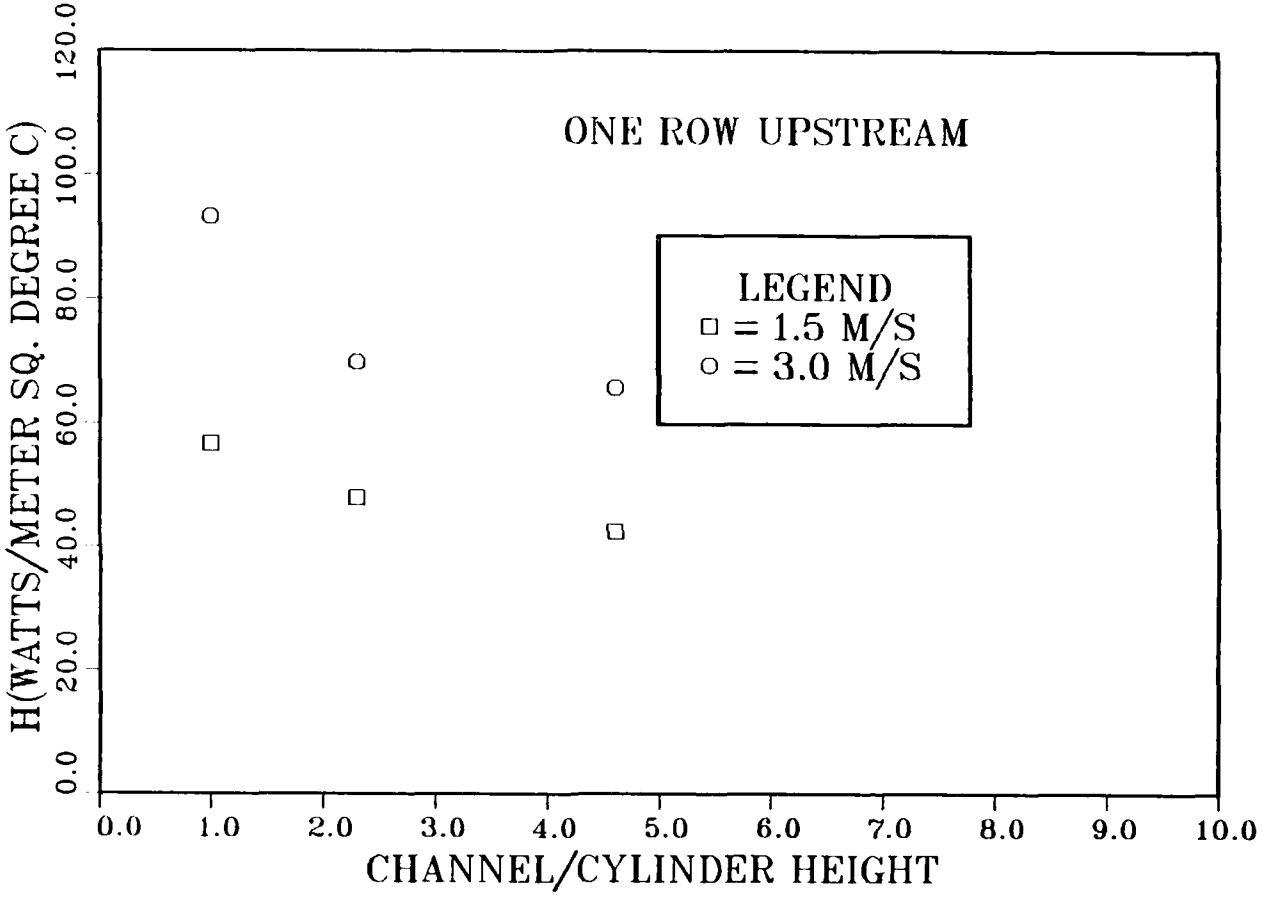

Figure 4.5 Heat-transfer Coefficient vs. Channel Height/ Cylinder Height Ratio With One Row Upstream.

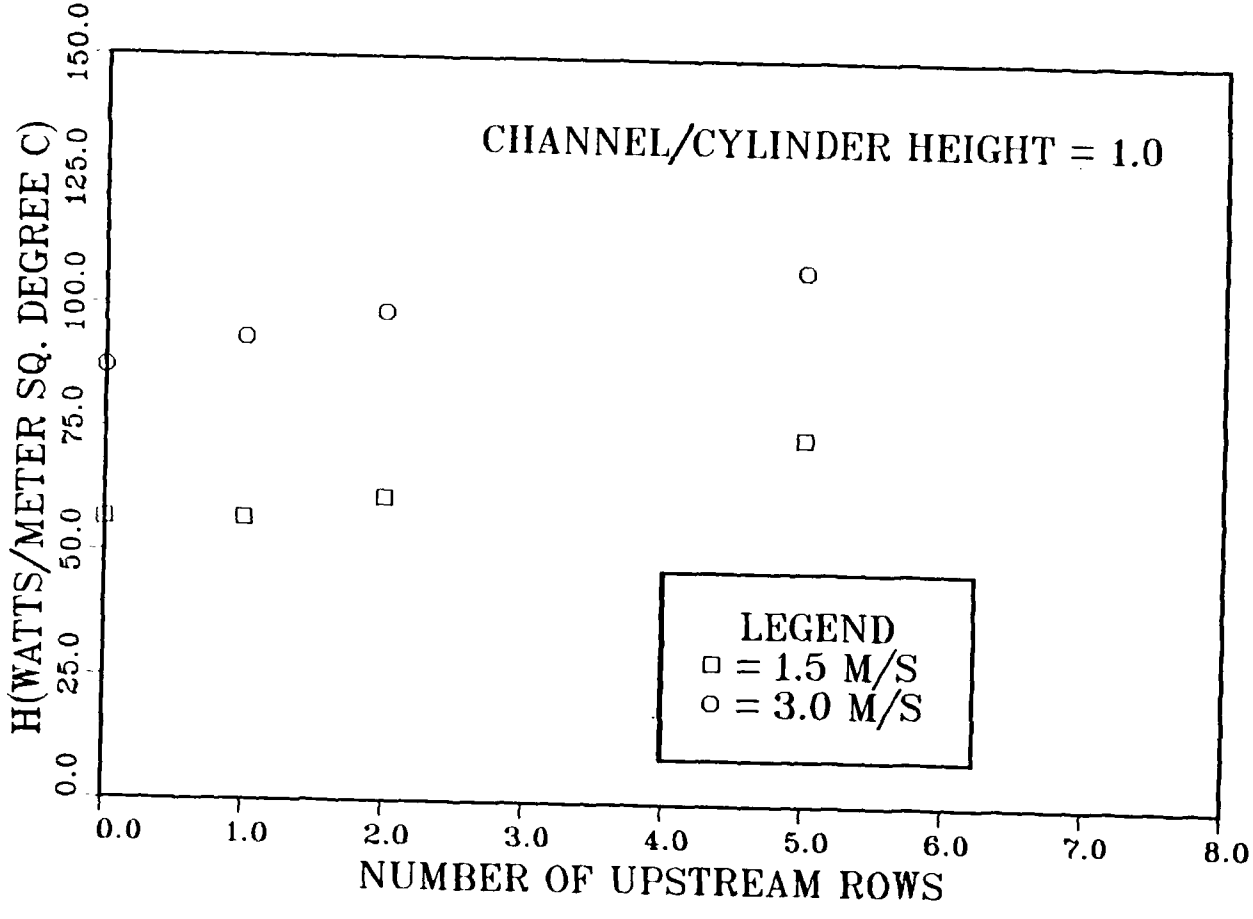

Figure 4.6 Heat-transfer Coefficient vs. Number of Upstream Rows for a Channel Height/Cylinder Height Ratio of 1.0.

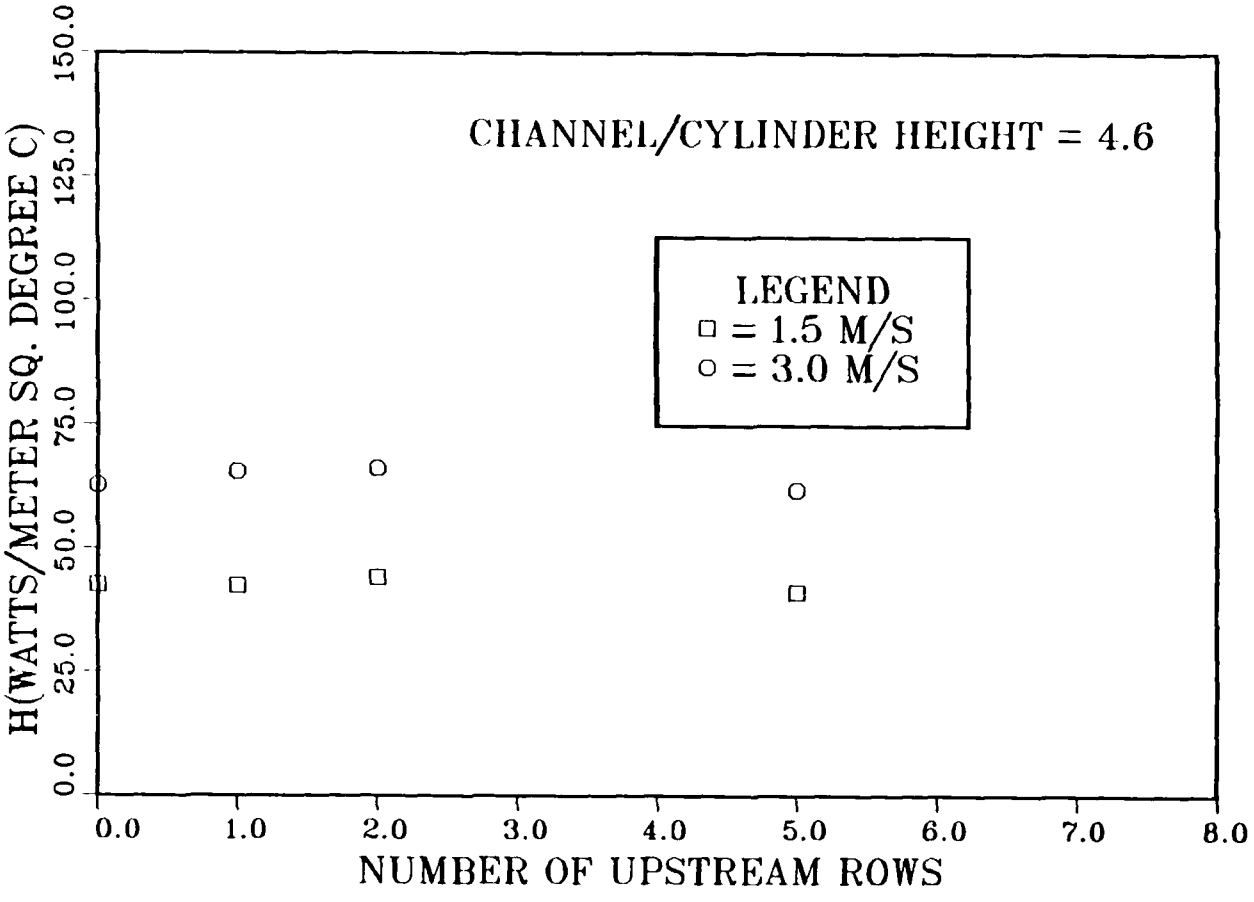

Figure 4.7 Heat-transfer Coefficient vs. Number of Upstream Rows for a Channel Height/Cylinder Height Ratio of 4.6.

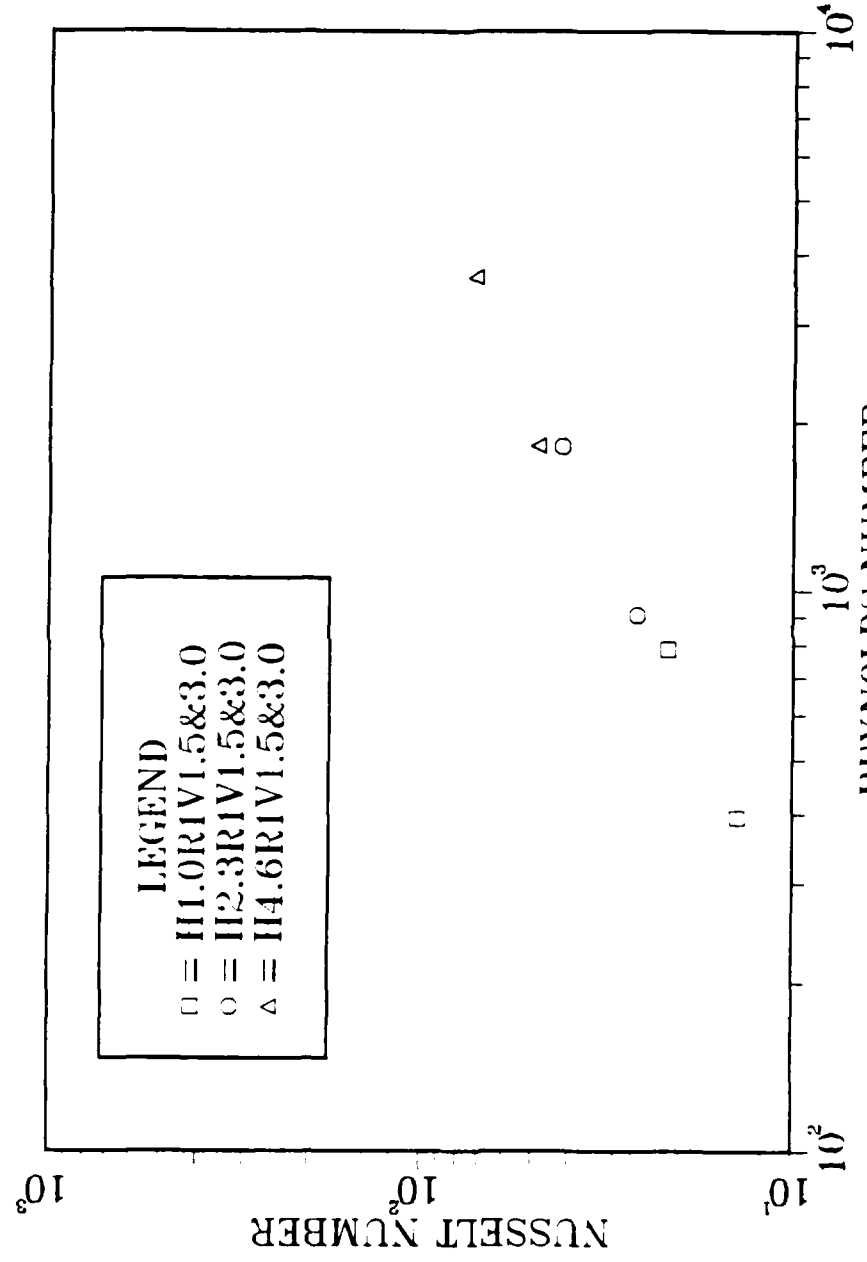

Figure 4.8 Nusselt Number vs. Reynold Number for all Three Channel Height to Cylinder Height Ratios.

V. CONCLUSIONS AND RECOMMENDATIONS

In this research, for cylindrical elements mounted in a vertical channel, the characteristic curves produced closely resemble those for a similar configuration of cubical elements which were investigated by of Arvizu and Moffat [Ref. 17].

Although there is room for more data to assist in making firm conclusions about the flow characteristics of air flow around cylinders, the

The following has been observed:

1. The 1/N characteristic curve produced by the thermal wake of a heated cylinder on an adiabatic wall in a channel, may allow for fairly accurate prediction of temperature increase in downstream elements in an array for various air flow rates.

2. Channel spacings and airflow rates have very little affect on the shape of the characteristic curve produced by the thermal wake of a heated cylinder in an array.

3. The position of a heated cylinder in an array, on an adiabatic wall in a channel, has a definite affect on its heat transfer characteristics. Elements requiring more cooling should be placed closer to the freestream air inlet. This would reduce effects created by the thermal wake of other cylinders.

4. Heat transfer in an array of cylindrical elements is mainly influenced by the air flow between the cylinders and slightly less by the turbulence in the air flow.

5. As the channel height to cylinder height increases, the amount of heat transfer that occurs decreases to an asymototic limit near a channel/cylinder height ratio of 1.6.

For continued work in this field, it is recommended that, a longer test surface with more rows of elements be utilized along

with higher velocities and various geometric shapes. All of this can be accomplished with only a few modifications to the equipment at hand.

APPENDIX A.

THERMOCOUPLE CALIBRATION

The thermocouples were all connected to a wooden framed switchboard which was connected by 10' wire leads to seven scanner boards mounted in the autodata nine data acquisition device. This combination was then calibrated as a complete unit in the calibration laboratory against five known temperatures:

66.02°F, 106.14°F, 127.615°F, 151.20°F and 200.42°F

Thermocouple readings follow:

1	66.3	106.4	127.9	151.3	200.5
2	66.3	106.5	128.0	151.3	200.6
3	66.2	106.5	128.0	151.2	200.4
4	66.3	106.5	128.0	151.3	200.6
5	66.1	106.4	127.9	151.2	200.4
6	66.2	106.4	127.9	151.2	200.4
7	66.1	106.2	127.8	151.1	200.3
8	66.2	106.4	127.8	151.3	200.4
9	66.1	106.2	127.7	151.0	200.2
10	66.2	106.4	127.8	151.2	200.4
11	66.8	106.9	128.5	151.8	201.0
12	66.8	107.0	128.5	151.8	200.9
13	66.7	106.8	128.3	151.6	200.8
14	66.7	107.0	128.4	151.8	201.0
15	66.6	106.8	128.3	151.6	200.7
16	66.7	106.8	128.3	151.7	200.8
17	66.5	106.7	128.0	151.4	200.7
18	66.7	106.8	128.2	151.6	200.8
19	64.5	106.6	128.0	151.4	200.7
20	64.2	106.8	122.6	152.4	199.3
21	66.2	106.4	128.0	151.3	200.4
22	66.3	106.5	128.0	151.3	200.5
23	66.1	106.3	127.9	151.2	200.4
24	66.2	106.5	128.0	151.3	200.5
25	66.0	105.3	127.8	151.2	200.3
26	66.2	106.5	127.8	151.2	200.4
27	66.0	106.2	127.1	151.0	200.2
28	66.1	106.2	127.7	151.1	200.2
29	66.0	106.2	127.7	151.1	200.3
30	66.3	106.5	127.8	151.2	200.1
31	66.3	106.4	127.8	151.2	200.4
32	66.3	106.5	128.0	151.4	200.6
33	66.2	106.3	127.9	151.4	200.6
34	66.3	106.5	128.0	151.4	200.6
35	66.3	106.5	127.9	151.2	200.4
36	66.3	106.5	128.0	151.4	200.5
37	66.3	106.5	127.9	151.3	200.5
38	66.4	106.5	128.0	151.3	200.6
39	66.3	106.4	127.9	151.2	200.4
40	66.6	106.7	128.2	151.6	200.7
41	66.5	106.6	128.1	151.5	200.7
42	66.6	106.8	128.4	151.6	200.9
43	66.6	106.7	128.2	151.5	200.8
44	66.7	106.8	128.4	151.6	200.8
45	66.5	105.8	128.2	151.5	200.7
46	66.6	106.8	128.3	151.6	200.8
47	66.5	106.7	128.2	151.6	200.7
48	66.7	106.7	128.2	151.6	200.7
49	66.6	106.6	128.0	151.5	200.7
50	66.4	106.5	128.1	151.4	200.5
51	66.3	106.4	127.9	151.3	200.6
52	66.4	106.6	128.2	151.4	200.7
53	66.3	106.6	128.1	151.4	200.6
54	66.4	106.6	128.2	151.4	200.7
55	66.4	106.6	128.0	151.4	200.6
56	66.4	106.6	128.3	151.5	200.7
57	66.4	106.5	128.0	151.4	200.6
58	66.6	106.6	128.2	151.4	200.6
59	66.5	106.6	128.1	151.4	200.6
60	66.2	106.8	128.0	151.3	200.4
61	66.2	106.7	128.0	151.4	200.5
62	66.3	107.1	128.2	151.4	200.6
63	66.3	106.8	128.0	151.3	200.6
64	66.3	106.9	128.2	151.4	200.6
65	66.3	106.8	128.1	151.4	200.6
66	66.3	106.8	128.1	151.4	200.6
67	66.4	106.9	128.3	151.5	200.7
68	66.3	106.8	128.1	151.5	200.7

A least squares fit program was developed to produce thermocouple corrections with the following result:

$$T_{actual} = M \times T_{measured} + B$$

THERMOCOUPLE 1	M=	1.0017233	B=	-0.4258300
THERMOCOUPLE 2	M=	1.0012808	B=	-0.4281250
THERMOCOUPLE 3	M=	1.0022497	B=	-0.4744628
THERMOCOUPLE 4	M=	1.0012808	B=	-0.4281250
THERMOCOUPLE 5	M=	1.0013457	B=	-0.2961913
THERMOCOUPLE 6	M=	1.0019846	B=	-0.3997558
THERMOCOUPLE 7	M=	1.0017433	B=	-0.2480956
THERMOCOUPLE 8	M=	1.0017471	B=	-0.3687988
THERMOCOUPLE 9	M=	1.0026321	B=	-0.3038086
THERMOCOUPLE 10	M=	1.0019560	B=	-0.3760253
THERMOCOUPLE 11	M=	1.0017424	B=	-0.9492187
THERMOCOUPLE 12	M=	1.0026770	B=	-1.0715818
THERMOCOUPLE 13	M=	1.0026207	B=	-0.9038085
THERMOCOUPLE 14	M=	1.0013180	B=	-0.8735839
THERMOCOUPLE 15	M=	1.0026846	B=	-0.8721191
THERMOCOUPLE 16	M=	1.0024166	B=	-0.8971679
THERMOCOUPLE 17	M=	1.0021400	B=	-0.6605957
THERMOCOUPLE 18	M=	1.0025959	B=	-0.8805175
THERMOCOUPLE 19	M=	1.0018959	B=	-0.6086425
THERMOCOUPLE 20	M=	0.9916704	B=	2.2940912
THERMOCOUPLE 21	M=	1.0018024	B=	-0.4160444
THERMOCOUPLE 22	M=	1.0019808	B=	-0.4994628
THERMOCOUPLE 23	M=	1.0011015	B=	-0.2445800
THERMOCOUPLE 24	M=	1.0013380	B=	-0.3956054
THERMOCOUPLE 25	M=	0.9986798	B=	0.3308593
THERMOCOUPLE 26	M=	1.0022001	B=	-0.4279296
THERMOCOUPLE 27	M=	1.0018101	B=	-0.0564453
THERMOCOUPLE 28	M=	1.0024242	B=	-0.2967773
THERMOCOUPLE 29	M=	1.0010777	B=	-0.1212890
THERMOCOUPLE 30	M=	1.0049429	B=	-0.7454101
THERMOCOUPLE 31	M=	1.0026007	B=	-0.4801757
THERMOCOUPLE 32	M=	1.0010719	B=	-0.4208984
THERMOCOUPLE 33	M=	0.9999380	B=	-0.1928710
THERMOCOUPLE 34	M=	1.0010719	B=	-0.4208984

THERMOCOUPLE 35	M=	1.0028639	B=	-0.5545898
THERMOCOUPLE 36	M=	1.0017776	B=	-0.4930175
THERMOCOUPLE 37	M=	1.0019627	B=	-0.4770995
THERMOCOUPLE 38	M=	1.0019207	B=	-0.5316894
THERMOCOUPLE 39	M=	1.0026245	B=	-0.5033203
THERMOCOUPLE 40	M=	1.0026214	B=	-0.7976074
THERMOCOUPLE 41	M=	1.0017195	B=	-0.6256835
THERMOCOUPLE 42	M=	1.0013046	B=	-0.7516601
THERMOCOUPLE 43	M=	1.0019274	B=	-0.7330077
THERMOCOUPLE 44	M=	1.0026417	B=	-0.9266112
THERMOCOUPLE 45	M=	0.9997830	B=	-0.2326660
THERMOCOUPLE 46	M=	1.0019027	B=	-0.8003417
THERMOCOUPLE 47	M=	1.0017757	B=	-0.6931152
THERMOCOUPLE 48	M=	1.0030603	B=	-0.9011718
THERMOCOUPLE 49	M=	1.0023384	B=	-0.7065917
THERMOCOUPLE 50	M=	1.0024405	B=	-0.6196777
THERMOCOUPLE 51	M=	1.0010166	B=	-0.3536133
THERMOCOUPLE 52	M=	1.0013094	B=	-0.5520507
THERMOCOUPLE 53	M=	1.0013409	B=	-0.4960937
THERMOCOUPLE 54	M=	1.0013094	B=	-0.5520507
THERMOCOUPLE 55	M=	1.0019588	B=	-0.5768066
THERMOCOUPLE 56	M=	1.0011234	B=	-0.5678222
THERMOCOUPLE 57	M=	1.0017183	B=	-0.5253417
THERMOCOUPLE 58	M=	1.0032902	B=	-0.8309081
THERMOCOUPLE 59	M=	1.0026283	B=	-0.7043456
THERMOCOUPLE 60	M=	1.0027475	B=	-0.6196288
THERMOCOUPLE 61	M=	1.0016108	B=	-0.4912597
THERMOCOUPLE 62	M=	1.0025406	B=	-0.7730468
THERMOCOUPLE 63	M=	1.0019932	B=	-0.5812500
THERMOCOUPLE 64	M=	1.0020733	B=	-0.6718749
THERMOCOUPLE 65	M=	1.0018148	B=	-0.5980468
THERMOCOUPLE 66	M=	1.0018148	B=	-0.5980468
THERMOCOUPLE 67	M=	1.0018339	B=	-0.7208007
THERMOCOUPLE 68	M=	1.0009155	B=	-0.5206543

Two plots of T actual vs Tmeasures for two thermocouples are presented in Figure A.1 and Figure A.2 to demonstrate their linearity.

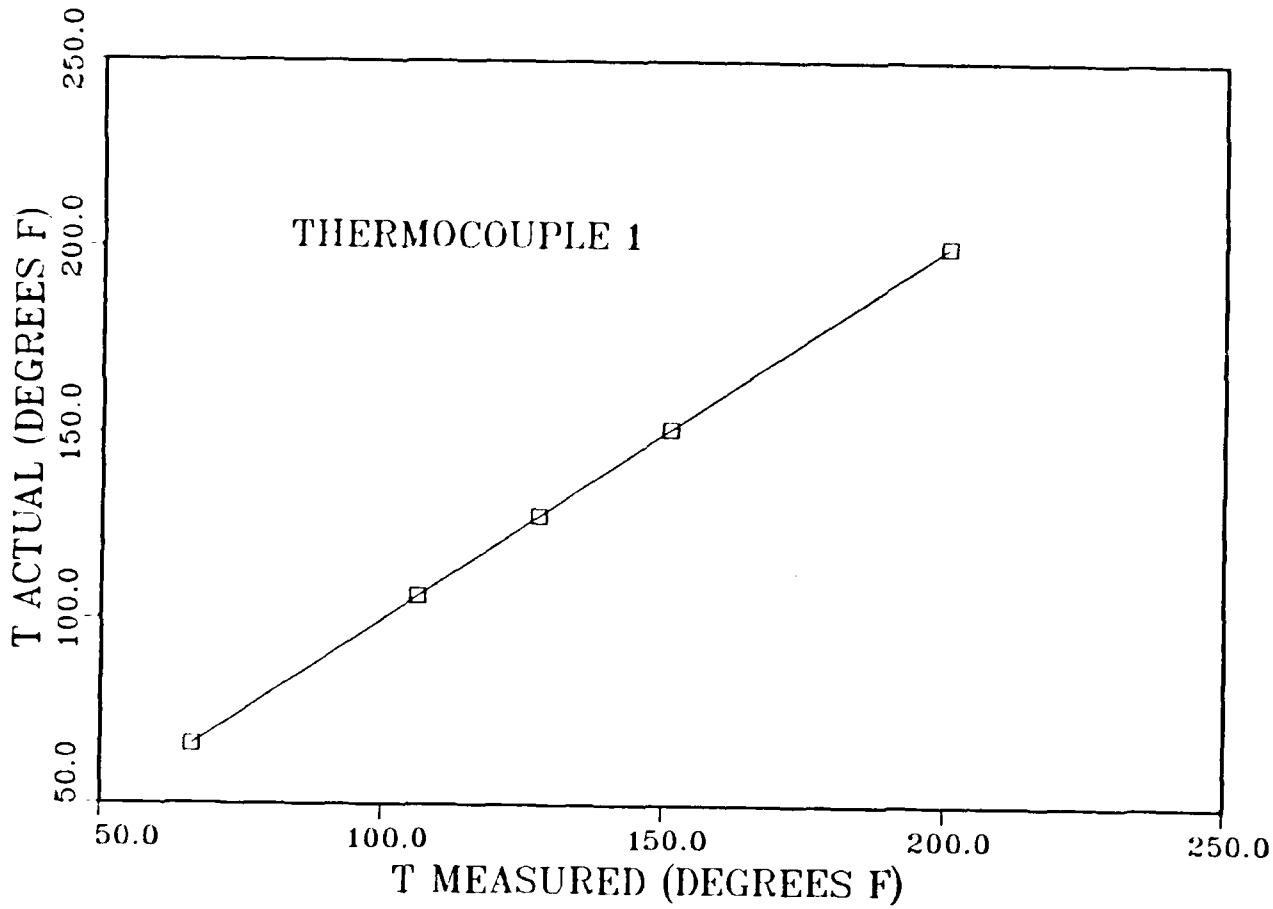
THERMOCOUPLE 1
T ACTUAL (DEGREES F)
50.0
100.0
150.0
200.0
250.0
T MEASURED (DEGREES F)
50.0
100.0
150.0
200.0
250.0

Figure A.1

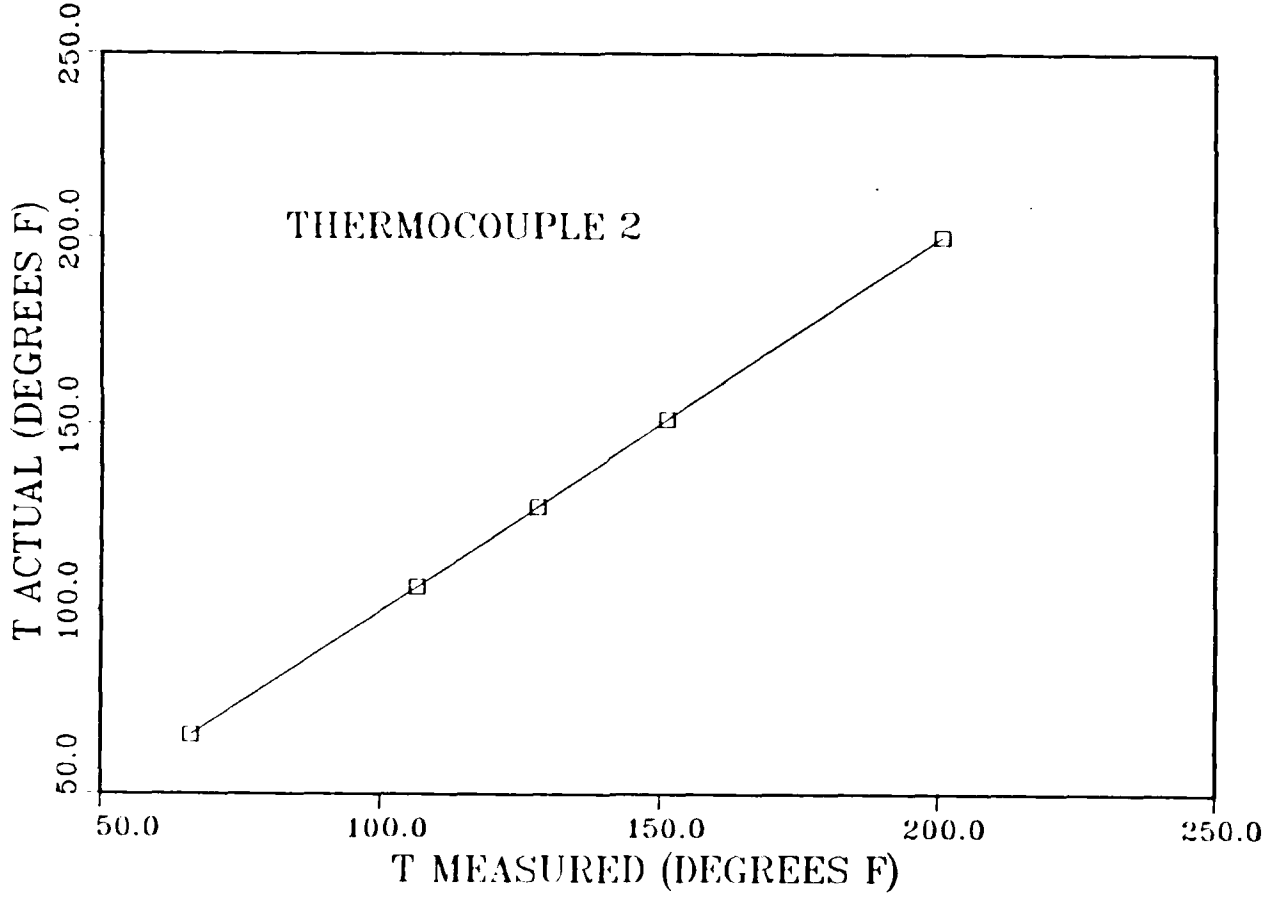
THERMOCOUPLE 2
T ACTUAL (DEGREES F)
50.0
100.0
150.0
200.0
250.0
T MEASURED (DEGREES F)
50.0
100.0
150.0
200.0
250.0

Figure A.2

APPENDIX B

TABULATED DATA

Heated Cylinder in the First Row

H = 1.0	1.5m/s	3.0m/s
Downstream Row No.	Theta	Theta
1	1.0	1.0
2	.468	.524
3	.336	.380
4	.251	.311
5	.181	.211

Heated cylinder in the first row.

H = 4.6	1.5m/s	3.0m/s
Downstream Row No.	Theta	Theta
1	1.0	1.0
2	.497	.484
3	.365	.380
4	.276	.277
5	.197	.185

Heated cylinder in the second row.

H = 2.3	1.5m/s	3.0m/s
Downstream Row No.	Theta	Theta
1	1.0	1.0
2	.501	.514
3	.324	.354
4	.250	.269

TABULATED DATA

Row No.	$T_{s,o}$(°C)	T (°C)	$\dot{Q}$(w)	h(w/m^2°C)	Re_H	Nu	U (m/s)
H=1.0							
1	98.5	20.3	3.03	56.61	394.2	14.09	1.5
2	98.9	20.3	3.05	56.71	394.2	14.11	1.5
3	99.6	20.5	3.28	61.16	393.9	15.21	1.5
4	97.6	20.0	3.18	60.34	394.5	15.02	1.5
6	96.3	20.1	3.74	73.87	394.4	18.39	1.5
1	101.2	20.8	4.59	87.27	787.2	21.69	3.0
2	89.4	20.7	4.17	93.26	787.4	23.19	3.0
3	78.9	20.5	3.73	98.52	787.9	24.51	3.0
4	96.8	20.2	4.74	95.26	787.6	23.71	3.0
6	86.2	20.3	4.57	107.69	788.3	26.80	3.0
H=2.3							
1	111.0	20.0	4.12	45.77	907.4	26.21	1.5
2	105.7	20.1	4.04	47.93	907.1	27.44	1.5
3	102.8	20.1	4.13	51.03	907.1	29.22	1.5
6	93.7	20.1	3.78	52.61	907.1	30.12	1.5
1	99.3	20.2	5.50	73.19	1813.7	41.90	3.0
2	110.1	20.1	5.99	69.86	1814.2	39.99	3.0
3	118.2	20.2	6.81	73.20	1813.7	41.90	3.0
6	71.8	20.1	3.91	80.03	1814.2	45.82	3.0
H=4.6							
1	96.7	20.0	3.27	42.74	1814.7	48.96	1.5
2	97.3	20.2	3.27	42.49	1813.7	48.65	1.5
3	104.8	20.3	3.71	44.20	1813.2	50.60	1.5
4	100.7	20.6	3.00	36.9	1811.6	42.22	1.5
6	91.5	20.6	2.92	41.14	1811.6	47.06	1.5
1	112.3	19.5	5.60	62.83	3634.7	72.04	3.0
2	99.6	19.8	5.02	65.70	3631.6	75.28	3.0
3	95.6	19.9	4.80	66.23	3630.6	75.87	3.0
4	91.2	20.1	3.92	56.91	3628.5	65.17	3.0
6	85.8	20.1	3.92	61.93	3628.5	70.91	3.0

LIST OF REFERENCES

1. Kraus, A.D. and Bar-Cohen, A., Thermal Analysis and Control of Electronic Equipment, New York: McGraw-Hill Book Co., 1983.

2. Elenbaas, W., "Heat Dissipation of Parallel Plates by Free Convection," Physics, 9(1), pp. 1-28, 1942.

3. Bodoia, J.R. and Osterle, J.F., "The Development of Free Convection Between Heated Vertical Plates," Trans. ASME J. Heat Trans., 84, pp. 40-44, 1962.

4. Engel, R.K. and Mueller, W.K., "An Analytical Investigation of Natural Convection in Vertical Channels," ASME paper 67-Ht-6, 1967.

5. Aung, W., Kessler, T.J., and Beitin, K.I., Natural Convection Cooling of Electronic Cabinets Containing Arrays of Vertical Circuit Cards, presented at the ASME Winter Annual Meeting, New York, New York, November 26-30, 1972.

6. Aung, W., "Heat Transfer in Electronic Systems With Emphasis on Asymmetric Heating," Bell System Tech. J., 52, July-August 1973.

7. Kelleher, M.D., "A Method to Predict the Thermal Performance of Printed Circuit Board Mounted Solid State Devices," Naval Electronics Lab Report No. NPS-59Kk 75071, Naval Postgraduate School, Monterey, California, July 1975.

8. Tamura, A., et al., "Packaging and Assembly of DIO Electronic Switching System and its Components," Kitachi Review, 22(7), pp. 305-315, 1971.

9. Finch, D.J, "Forced Air Cooling of Dual-in-line Packages," Marconi Review, 35(184), 1972.

10. Laermer, L., "Air Through Hollow Cards Cools High-Power LSI," Electronics, pp. 113, 118, June 13, 1974.

11. Marto, P.J., "The Thermal Performance of Air Cooled Circuit Boards Used in Standard Electronic Package Designs," Naval Electronics Lab Report No. NPS-59Mx 74051, Naval Postgraduate School, Monterey, California, 93943-5100, May, 1974.

12. Parkes, J.F. and Preston, S.B., "Cooling Integrated Circuits in Computers," Electronics and Power, April 3, 1975.

13. Dipprey, D.F. and Sabersky, R., "Heat and Momentum Transfer in Smooth and Rough Tubes at Various Prandtl Numbers," Int. J. Heat Mass Transfer, 6, pp. 329-353, 1963.

14. Kader, B.A. and Yaglom, A.M., "Turbulent Heat and Mass Transfer from a Wall with Parallel Roughness Ridges," Int. J. Heat Mass Transfer, 20, pp. 345-357, 1977.

15. Owen, P.R. and Thomson, W.R., "Heat Transfer Across Rough Surfaces," J. Fluid Mech., 15, pp. 321-334, 1963.

16. Kraus, A.D., Heat Transfer Software, New York: McGraw-Hill Book Co., 1986.

17. Arvizu, D.E. and Moffat, R.J., "Experimental Heat Transfer From an Array of Heated Cubical Elements on an Adiabatic Channel Wall," Report No. HMT-33, Dept. of Mechanical Engineering, Stanford University, Stanford, California, 1981.

18. Ortega, A., Exreriments on Buoyancy-Induced Convection Heat Transfer From an Array of Cubical Elements on a Vertical Channel Wall, Ph.D. Dissertation, Dept. of Mechanical Engineering, Stanford University, Stanford, California, 1986.

INITIAL DISTRIBUTION LIST

		No. Copies
1.	Defense Technical Information Center Cameron Station Alexandria, Virginia 22304-6145	2
2.	Library, Code 0142 Naval Postgraduate School Monterey, California 93943-5000	2
3.	Dr. A. J. Healey Department Chairman, Code 69 Department of Mechanical Engineering Naval Postgraduate School Monterey, California 93943-5000	1
5.	Dr. Allan D. Kraus, Code 69Ks Department of Mechanical Engineerng Naval Postgraduate School Monterey, California 93943-5000	3
7.	Commanding Officer Attn: LT James D. Piatt, Jr. Puget Sound NSYD Bremerton, Washington 98314	2
8.	Prof. Robert Moffat Thermosciences Division Mechanical Engineering Department Stanford University Stanford, California 94350	1

END

2-87

DTIC